# CHAPTER VI

# IN VITRO AND IN VIVO BIOLOGICAL EVALUATION OF SILVER-CONTAINING ELECTROSPUN FIBROUS MEMBRANES FOR TISSUE ENGINEERING AND WOUND DRESSING APPLICATIONS

## 6.1 Abstract

This study was designed to determine the in vitro and in vivo biocompatibility of e-spun fibrous membranes of gelatin and gelatin that contained 0.75-2.50% silver nitrate ($AgNO_3$) or silver nanoparticles (Agnano) and poly(L-lactic acid) (PLLA), polycaprolactone (PCL) and 1,6-disiocyanatohexane-extended poly(1,4-butylene succinate) (PBSu-DCH) biodegradable aliphatic polyesters. In vitro human monocyte/macrophage cultures were used with the MTT test for cell viability and confocal microscopy to determine the adherent cell density on the respective materials at day 0 (2h), 3, 7 and 10. Statistical analyses were performed comparing the results of e-spun fibrous membranes of gelatin containing 0.75-2.50%$AgNO_3$ or Agnano at each time point with e-spun gelatin fibrous membranes. Only the 0.75%Agnano e-spun fibrous membranes were statistically comparable to the e-spun gelatin fibrous membranes. Based on the adherent cell density and cell viability data, all other $AgNO_3$ and Agnano were considered to be non-biocompatible or toxic. Statistical analysis demonstrated that the Agnano materials were less toxic than the $AgNO_3$ materials. In vitro adherent cell density and cell viability results showed that the three polyesters were statistically comparable and biocompatible.

For the in vivo study, samples of the materials were subcutaneously implanted in rats for 7, 14, and 28 days. After sacrifice, the tissue implant sites were histologically evaluated for inflammatory, foreign body reaction, and wound healing responses. Results from the in vivo studies were comparable to those from the in vitro studies with the e-spun gelatin fibrous membranes and the 0.75%Agnano demonstrating the earliest rapid resolution of the acute and chronic inflammatory responses with mild foreign body reactions and mild to moderate fibrous capsule formation at 14 and 28 days. The three polyester materials demonstrated

biocompatibility with comparable inflammatory, foreign body reaction, and wound healing responses. As expected, the polyester materials demonstrated early evidence of biodegradation.

(Keywords: Biocompatibility, Silver-containing e-spun fibrous membrames, E-spun gelatin fibrous membranes, E-spun polyester fibrous membranes)

## 6.2 Introduction

The development of novel biomaterials, biomedical devices or tissue engineered constructs requires a thorough understanding of the biological responses to the materials upon their implantation. In response to the implantation, the host tissue undergoes a sequence of events: injury, cellular infiltration, acute inflammation, chronic inflammation, granulation tissue, foreign body reaction (FBR), and fibrous capsule formation [1]. Injury also results in infiltration of cells to the site of the implant, setting off inflammation and wound healing events. Acute inflammation occurs over a short period of days where polymorphonuclear cells (PMNs) predominate and act to phagocytose and eliminate pathogens and foreign particles. PMNs of acute inflammatory phase are replaced by monocytes, macrophages, plasma cells and lymphocytes as the response progresses to chronic inflammation. The extent of these responses determines the biocompatibility of the implant materials. Implantation of synthetic biomaterials also elicits a foreign body reaction consisting of monocyte adhesion, differentiation to macrophages and subsequent macrophage fusion to form foreign body giant cells (FBGCs) [2-7].

Concurrent to the events in the region around the implant is the series of events at the material/tissue interface called the foreign body reaction. The fusion of macrophages to form FBGCs occurs in an attempt to remove the offending foreign material and can persist for the lifetime of the implant. FBGCs have been shown to mediate degradation of biomaterial surfaces through the release of reactive oxygen intermediates (ROIs, oxygen free radicals), degradative enzymes and acid into the privileged zone between the cell membrane and biomaterial surface [8-9]. As the tissue around the implanted material progresses to the healing response, granulation

tissue forms involving neovascularization and progressive increase in fibroblast activity. Fibroblasts proliferate and the synthesis of extracellular matrix (ECM) increases to support the healing, thus the formation of new tissue at the implant site. Granulation tissue is the precursor to fibrous capsule formation and it is separated from the implant or biomaterial by the cellular components of the foreign body reaction [5,6].

Normally, cells most likely do not interact directly with the foreign material but rather they recognize the implanted material via the layer of absorbed proteins on the surface [10,11]. The adsorbed blood protein-modified material surface is the substrate with which the recruited monocytes/macrophages encounter and interact. Monocytes/macrophages play an integral part in not only the inflammation and wound healing responses at the implant site but also the tissue response at the tissue/material interface. Monocytes migrate from the blood circulation to the implantation site, adhere to the surface of a biomaterial and differentiate into macrophages to initiate the foreign body reaction [4-7]. The inflammatory, wound healing and foreign body responses can all act to determine whether an implant such as a tissue-engineered scaffold will fail or be able to perform its intended functions.

In recent years, electrospinning process has attracted a great deal of attention due to its ability to produce ultrafine fibers with diameters in the nano- to micrometer range [12]. Because of their physical uniqueness (e.g., a high surface area to mass or volume ratio, a small inter-fibrous pore size with a high porosity of the fiber mat), the proposed use for electrospun (e-spun) polymeric fibers is in areas such as filtration [13-14], optical and chemical sensors [15-17], electrode materials [18-20], and biomedical fields [21-23]. Some potential uses of e-spun fibrous membranes in biomedical fields are, for example, immobilization of enzymes [24], tissue-engineered scaffolds [25,26], wound dressing materials [27-31] and delivery carriers for DNA [32] and drugs [33-36]. For a successful application to a specific target, the e-spun fibrous scaffolds must exhibit suitable physical and biological properties closely matching the desired requirements. For example, in tissue engineering, the e-spun fibrous scaffolds should physically resemble the fibrous features of the ECM with suitable mechanical integrity [37]. It should also be able to promote cell adhesion, spreading and proliferation. For wound dressing, the e-spun

fibrous scaffolds should not only serve as substrates for tissue regeneration, but also may deliver suitable bioactive agents, including drugs (e.g., antibiotic agent such as silver nanoparticles [28,29]), in a controlled manner during healing. The fabrication of such functional e-spun fibrous scaffolds for biomedical applications often requires an approach combining physics (e.g., mechanical modulus and strength), chemistry (e.g., hydrophilicity), biology (e.g., biodegradability and biocompatibility) and engineering.

Most importantly, the basic requirements for materials with intended uses in tissue engineering and wound dressing are biocompatibility and biodegradability. Among the many biodegradable polymers, various polyesters, such as polycaprolactone (PCL) [38-42], poly(L-lactic acid) (PLLA) [43-44], poly(glycolic acid) (PGA) [46,47], poly(3-hydroxybutyrate) (PHB) [48], poly(3-hydroxybutyrate-co-3-hydroxyvalerate) (PHBV) [48,49], and poly(butylene succinate) (PBSu) [50], have attracted a great deal of attention. They can be used as bone scaffolding materials owing to their potentially hydrolysable ester bonds and their slow degradation rate that are suitable for bone regeneration. E-spun fibrous membranes of poly(ethylene-co-vinyl alcohol) [51], collagen [52], gelatin [53], polyurethane [54], chitin and chitosan [55], cellulose acetate [56] and silk fibroin [57] have been investigated for use as wound dressings. Historically, certain polyesters (e.g., PCL, PLLA, PGA, PHB, PHBV and PBS) and proteins (e.g., collagen, gelatin, chitin and chitosan) in the form of e-spun fibrous membranes have been investigated for the in vitro responses with a number of cell lineages, such as human osteoblasts (SaOS-2) [38,50], human dermal fibroblasts [40], mouse fibroblasts (L929) [50,55], neural stem cells (NSCs) [44], Schwann cells [48] and normal human keratinocytes [52]. However, detailed investigations on biocompatibility and immune responses in vivo (i.e., inflammation and wound healing responses) of these biomaterials are still lacking. It is, therefore, our intention to comprehensively study and report in vitro and in vivo biological evaluation of e-spun fibrous membranes of some of the mentioned materials with intended uses as tissue scaffolds and/or wound dressings.

In the present contribution, the e-spun fibrous membranes of gelatin and gelatin that contained silver nitrate ($AgNO_3$)/silver nanoparticles (Agnano), poly(L-lactic acid) (PLLA), polycaprolactone (PCL) and 1,6-diisocyanatohexane-extended

poly(1,4-butylene succinate) (PBSu-DCH) were evaluated for their in vitro and in vivo biocompatibility. The in vitro response of monocytes with various types of e-spun fibrous membranes has been evaluated. The cell viability and the adherent cell density on e-spun fibrous membranes were investigated by using MTT assay and Confocal microscopy, respectively. Additionally, in vivo tissue responses were also investigated by subcutaneously implanting these e-spun fibrous membranes in rats with subsequent histological evaluation.

## 6.3 Materials and methods

### 6.3.1 Materials

Gelatin powder (type A; porcine skin; 170-190 Bloom) was purchased from Fluka (Switzerland). Silver nitrate ($AgNO_3$; 99.998% purity) was purchased from Fisher Scientific (USA). Glacial acetic acid ($CH_3COOH$) was purchased from Mallinckrodt Chemicals (USA). An aqueous solution of glutaraldehyde (GTA; 5.6 M or 50 vol.%) was purchased from Fluka (Switzerland). Poly(L-lactic acid) (PLLA; Mw = 80,000g/mol), polycaprolactone (PCL; Mw = 80,000g/mol) and poly (1,4-butylene succinate) extended with 1,6-diisocyanatohexane (PBSu-DCH; Mw = 412.4g/mol) were purchased from Sigma-Aldrich (USA). Dichloromethane (DCM) Analytical Reagent ($CH_2Cl_2$; Fisher Scientific, UK), *N,N*-dimethylformamide (DMF) Analytical Reagent ($C_3H_7NO$; Lab Scan), trifluoroacetic acid (TFA) ($C_2HF_3O_2$; Fluka, Switzerland) are used as a solvent. All chemicals and reagents were used without further purification.

### 6.3.2 Preparation of electrospun fibrous membranes

#### *6.3.2.1 Preparation of neat, $AgNO_3$- and Agnano-containing e-spun fibrous membranes*

$AgNO_3$ or Agnano was first dissolved in a quantity of 70:30 v/v glacial acetic acid/distilled water. A metered weight of gelatin powder was then added into the as-prepared $AgNO_3$ solution. Slight stirring was used to expedite the dissolution and homogenize the solution. The concentration of the base gelatin solution was fixed at 22% w/v (based on the volume of the mixed solvent) and the amount of $AgNO_3$ or Agnano was varied at 0.75, 1.00 and 2.50% w/w (based on the

weight of the gelatin powder) [28]. The Agnano particles used in this work were synthesized according to a method proposed by He et al. [58] using $NaBH_4$ as the reducing agent.

The base gelatin solution and the 0.75, 1.00 and 2.50% $AgNO_3$-containing gelatin solutions that had been aged for 12 hr were fabricated into neat and $AgNO_3$-containing gelatin fibrous membranes by e-spinning. The 0.75, 1.00 and 2.50%Agnano-containing gelatin solutions that had been stirred for 1 hr were fabricated into Agnano-containing gelatin fibrous membranes by e-spinning, Each of the as-prepared solutions was loaded in a standard 10-mL glass syringe, the open end of which was attached with a blunt gauge-20 stainless steel hypodermic needle (OD = 0.91 mm), used as the nozzle. Both the syringe and the needle were tilted ~45°C from a horizontal baseline. A piece of aluminum (Al) sheet wrapped around a rotating cylinder (OD and width ≈ 15 cm; ~50-60 rpm) was used as the collecting device. A Gamma High-Voltage Research ES30P-5W DC power supply (Florida, USA) was used to charge the solution by attaching the emitting electrode of positive polarity to the nozzle and the grounding one to the collecting device. A fixed electrical potential of 15 kV was applied across a fixed distance between the tip of the needle and the outer surface of the collecting device (i.e., collection distance, measured at right angle to the surface of the collecting device) of 20 cm. The e-spun fiber mats were collected continuously for 48 hr. The thickness of the neat, the $AgNO_3$- and Agnano-containing gelatin fiber mats were measured by a Mitutoyo digital micrometer. The thickness of these fiber mats were 200±20 μm.

Cross-linking of the neat, the $AgNO_3$- and the Agnano-containing gelatin fibrous membranes was carried out by clamping each of the fiber mat samples between a pair of supporting stainless steel frames (4.5 cm × 10 cm) with adhesive tapes in a sealed chamber saturated with the vapor from 20 ml of the as-received GTA aqueous solution. The temperature of the chamber was maintained at 37°C and each fiber mat sample was exposed to the moist GTA vapor for 0.5 hr. After exposure, the sample was heat-treated in a heating oven at 110°C for 24 h to enhance the cross-linking reaction and to remove moisture and the unreacted GTA.

*6.3.2.2 Preparation of poly(L-lactic acid) (PLLA), polycaprolactone*

*(PCL) and poly (1,4-butylene succinate) extended with 1,6-diisocyanatohexane (PBSu-DCH) e-spun fibrous membranes*

E-spun PLLA, e-spun PCL and e-spun PBSu-DCH were prepared by e-spinning from a 10% w/v PLA solution in 7:3 v/v DCM/DMF [59], a 12% w/v PCL solution in 50:50 v/v DCM/DMF [38] and a 22% w/v PBSu-DCH in 90:10 v/v DCM/TFA [50], respectively. The as-prepared PLLA, PCL and PBSu-DCH solution was contained in a glass syringe, the open end of which was connected to a blunt gauge-20 stainless steel hypodermic needle (OD = 0.91 mm) used as the nozzle. Both the syringe and the needle were tilted ~45°C from a horizontal baseline. An Al sheet wrapped around a rotating cylinder (OD and width ≈ 15 cm; ~50-60 rpm) was used as the collector. The distance from the tip of the needle to the surface of the Al sheet defining the collection distance was fixed at 18 cm (e-spun PLA), 10 cm (e-spun PCL) and 20 cm (e-spun PBSu-DCH). A gamma high-voltage research D-ES30PN/M692 power supply was used to generate a high dc potential (i.e., 20 kV (e-spun PLLA), 21 kV (e-spun PCL) and 22 kV (e-spun PBSu-DCH). The emitting electrode of positive polarity was connected to the needle, while the ground electrode was connected to the collector. The e-spun fiber mats were collected continuously for 24 hr. The thickness of these fiber mats were measured by a Mitutoyo digital micrometer and were 180±20 μm.

6.3.3 Sterilized materials for in vitro and in vivo study

Materials were immersed in 0.1% Triton X-100 and sonicated for 10 min and then washed twice with sterilized distilled water. Materials were then placed in sterile 24-wells plates sterilized with 70% ethanol for 30 min and washed twice with sterile phosphate-buffered saline without $Ca^{++}$ and $Mg^{++}$ ($PBS^{--}$, GIBCO). Materials were air-dried under sterile conditions.

6.3.4 In vitro study

In vitro studies utilizing the MTT test for cell viability and confocal microscopy to determine the adherent cell density on the respective materials were carried out. In vitro specimens with adherent cells were evaluated at Day 0 (2h), Day 3, Day 7 and Day 10.

*6.3.4.1 Monocyte isolation and culture*

Peripheral blood monocytes were isolated from healthy adult blood donors by a non-adherent centrifugation method utilizing a Percoll gradient as previously described [5]. Separated monocytes was washed twice with phosphate-buffered saline with $Ca^{++}$ and $Mg^{++}$ ($PBS^{++}$, GIBCO), resuspended in serum free media (SFM, InVitrogen, Grand Island, NY) supplemented with L-glutamine, antibiotics and antimycotics, and kept at 4°C prior to plating. Before monocyte plating, materials were immersed in phosphate-buffered saline without $Ca^{++}$ and $Mg^{++}$ ($PBS^{--}$, GIBCO) overnight in order to allow the materials to become completely swollen. Monocytes were plated on the different materials in 24-well plates and modified with RGD (Fibronectin-like protein polymer; Sigma-Aldrich USA) as control. Cells were plated at $1x10^6$ cells per well in 0.5 ml per well of serum-free medium (SFM, InVitrogen, Grand Island, NY) supplemented with 20% autologus serum and incubated at 37°C with 5% $CO_2$. After 2h, the medium was replaced in 1 ml per well with fresh SFM and cells were re-incubated at 37°C with 5% $CO_2$ for 3, 7 and 10 days. On day 3, the medium in plate day 7 and day 10 were replaced with the same volumes of SFM supplemented with 5% heat-treated (56°C for 1h) autologus serum/95% SFM and re-incubated at 37°C with 5% $CO_2$. On day 7, the same medium exchange was carried out.

*6.3.4.2 MTT assay*

The viability of the cells cultured at each time point was determined with the 3-(4,5-dimethylthiazol-2-yl)-2,5- diphenyltetrazolium bromide (MTT) assay (R&D Systems Inc., Minneapolis, USA), with the viability of the cells cultured in 24-wells plate modified with RGD used as control. The MTT assay is based on the reduction of the yellow tetrazolium salt to purple formazan crystals by dehydrogenase enzymes secreted from the mitochondria of metabolically-active cells. The amount of purple formazan crystals formed is proportional to the number of viable cells. First, 0.5 ml of culture medium was aspirated and replaced with 50 μL/well of MTT solution for a 24-wells plate. Secondly, the plate was incubated for 2 hr at 37°C with 5% $CO_2$. The solution was then aspirated and 0.5 ml/well of DMSO was added to dissolve the formazan crystals. Finally, after 3 min of rotary agitation, the absorbance at the wavelength of 550 nm representing the viability of

the cells was measured using an EL808 Ultra Microplate Reader (BIO-TEK INSTRUMENTS, INC.)

*6.3.4.3 Confocal Microscopy*

Each time point, the cells on materials were fixed for 20 min with 3.7%formaldehyde and washed with phosphate-buffered saline with $Ca^{++}$ and $Mg^{++}$ ($PBS^{++}$, GIBCO). Cells were permeabilized with 0.5%Triton X-100 for 2 min and washed with $PBS^{++}$ and then incubated with *RNAse* (Ribonuclease A) (100 μg/ml) for 1.5h at 37°C with 5% $CO_2$. After that, the cells were stained with Alexa Fluor® 568 phalloidin (InVitrogen, Grand Island, NY) diluted 1:100, and YO-YO-488 (InVitrogen, Grand Island, NY) diluted 1:10,000 that was added 0.5 ml/well for 1 hour at room temperature and washed with $PBS^{++}$. Finally, the stained cells on the respective materials were held by using cover glass slips.

6.3.5 In vivo study

*6.3.5.1 Surgical implantation*

All procedures were approved by the Institutional Animal Care and Use Committee (IACUC) and NIH Animal Care Guidelines of Case Western Reserve University and used as described in a previously published protocol [60]. Samples of each materials (1 x 2 cm, n=2) were implanted subcutaneously, two per animal, in the posterior back areas of female Sprague-Dawley rats 12 weeks old (Charles Rivers Laboratories, North Wilmington, MA). Aerrane (Baxter, Deerfield, IL) was used in a continuous analgesic steam to keep the animals unconscious during implantation. The rats were shaved and their skin scrubbed with surgical grade Betadine (The Purdue Frederick Co., Stamford, CT). An incision 1.0-1.5 cm long was made in the skin about 2 cm above the tail and along the midline. Blunt dissection was used to prepare an implant pocket in the facial plane beneath the paniculous carnosus muscle from the underlying tissue from the incision to just above the hip. The sterilized material was then introduced through the incision and positioned within the pocket and away from the incision site. The incision was then closed with 9 mm stainless steel surgical wound clips (Becton Dickinson, Spark, MD) and washed with Betadine. Then, 0.5% Marcaine solution (Abbott Laboratories, North Chicago, IL), a local anesthetic, was applied onto the incision to minimize post-operative discomfort. Sterile surgical techniques were observed. In

this study, sterilized e-spun gelatin fibrous membranes were implanted into the rats as controls. The rats were maintained on Purina Rat Chow and water adlibitum at the Animal Research Facilities of Case Western Reserve University on 12 h light/dark cycles.

*6.3.5.2 Histological Evaluation*

Histological analysis was performed on the explanted tissue at 7, 14, and 28 days using a previously described protocol [61]. Following carbon dioxide euthanasia, the tissue enclosing the implant was carefully removed (5 x 5 cm), the fibrous capsule exposed, and the tissue samples pinned into a paraffin block submerged into 10% buffered formalin solution (Fisher Scientific, Fair Lawn, NJ). The material with the fibrous capsule surrounding it was cut into 2-3 mm wide sections that were embedded into paraffin blocks. Sections of 4 μm thickness then were cut and mounted onto slides. The slides were stained with either Hematoxylin and Eosin (H&E) or Masson's Trichrome (University Hospital of Cleveland, Histopathology Laboratory, Cleveland, OH). The stained sections were visualized using the Nikon-ACT Software Imaging System® (Nikon Corporation, Melville, NY) and photographs of all sections were taken.

Each section was scored on all phases of the inflammatory and wound healing response (acute inflammatory, chronic inflammatory, granulation tissue, and foreign body reaction), and fibrous capsule structure (organization, density, and vascularization). The qualitative characterization of the fibrous capsule structure employed analysis of H&E, as well as Masson's Trichrome stained tissue sections. The scoring system assigned a number, from 0 to 4, to each section at each time point, where 0 = none, 1 = minimal, 2 = mild, 3 = moderate, and 4 = extensive. Each section was scored using comparative analysis of explanted tissue at the same time point.

In this animal model, early time point (day 7) are normally characterized by acute or chronic inflammation, limited granulation tissue and foreign body reaction. At late time points (day 28), acute and chronic inflammatory are absent, while granulation tissue has significantly decreased from peak values usually reached by 21 days.

In determining the performance of the e-spun fibrous membranes of gelatin and gelatin that contained silver nitrate ($AgNO_3$) or silver nanoparticles (Agnano), poly(L-lactic acid) (PLLA), polycaprolactone (PCL) and 1,6-diisocyanatohexane-extended poly(1,4-butylene succinate) (PBSu-DCH) against competing constructs, the fibrous capsule structure and inflammatory and wound healing responses described above were summarized, for each sample at each time point, allowing for a comprehensive characterization of the in vivo behavior of these materials.

6.3.6 Statistical analysis

Multiple human donors were utilized to account for donor variability. In vitro studies, all results were obtained by repeating experiments 5 times utilizing different donors and presented as an average ± the standard error of the mean (n=5). Statistical analysis was preformed utilizing the student's two-tailed t-test on StatView™ software (JMP Software, Cary, NC). A *p*-value of less than 0.05 was considered statistically significant.

## 6.4 Results

### 6.4.1 In vitro study

#### *6.4.1.1 Cell viability and monocyte adhesion*

We utilized the MTT assay and immunocytochemical staining approach with confocal microscopy to quantitatively evaluate monocyte viability and adhesion on the material surfaces, respectively. All surfaces were examined after Day 0 (2h), Day 3, Day 7 and Day 10. In this study, the RGD-peptide coated on 24-well plates was used to ensure the cell plating methods in the MTT assay were working because of their general irrelevance beyond use as positive controls. A majority of the in vitro results were significant ($p < 0.05$) between materials compared within the same time point using the student's two-tailed t-test.

In general, cell viability and adherence were seen to decrease over time. Cell viability and adherence were nearly always highest on the surfaces of the e-spun gelatin fibrous membranes initially and then showed a marked decrease until the 10 day time point. Although different donors displayed different cell

viabilities and adherent cell densities, they all showed similar kinetics over time as moderately decreasing exponential curves. Day 0 (2h) and Day 3 trends showed the cell viability and adherence occurring in a similar ranking order: gelatin ~ 0.75%Agnano > 1.00%Agnano >> 0.75%$AgNO_3$ > 2.50%Agnano > 1.00%$AgNO_3$ > 2.50%$AgNO_3$. Day 7 trends showed the cell viability and adherence occurring in the following rank order: gelatin ~ 0.75%Agnano > 1.00%Agnano >> 2.50%Agnano > 0.75%$AgNO_3$ ~ 1.00%$AgNO_3$ ~ 2.50%$AgNO_3$. Day 10 trends showed the following rank order: gelatin ~ 0.75%Agnano > 1.00%Agnano >> 0.75%$AgNO_3$ ~ 1.00%$AgNO_3$ ~ 2.50%$AgNO_3$ ~ 2.50%Agnano. These changes over time can be seen in Figures 6.1a and 6.2a

The percentage of cell viability of the e-spun fibrous membranes of gelatin and gelatin that contained $AgNO_3$ or Agnano over time can be seen in Figure 6.3a. At day 0 (2h), the cell viability of e-spun gelatin fibrous membranes (~98%) was similar to the control, while the 0.75%Agnano and 1.00%Agnano-loaded e-spun gelatin fibrous membranes presented cell viability ranging between ~94% and ~67%, respectively. The cell viability was ~59%, and ~52% for the 0.75%$AgNO_3$ and 2.50%Agnano-loaded e-spun gelatin fibrous membranes, respectively. The 1.00-2.50%$AgNO_3$ e-spun gelatin fibrous membranes showed ~46% and ~23% cell viability, respectively. At day 3, the e-spun gelatin fibrous membranes showed ~83% cell viability, while the 0.75-2.50%Agnano-loaded e-spun gelatin fibrous membranes presented at ~76%, ~55% and ~29%, respectively. The cell viability of the 0.75-2.50%$AgNO_3$-loaded e-spun gelatin fibrous membranes was ~33%, ~23% and ~17%, respectively. At day 7, the cell viability of the e-spun gelatin fibrous membranes remained at ~74%, while the 0.75-2.50%Agnano-loaded e-spun gelatin fibrous membranes showed ~66%, ~49% and ~25% cell viability. For the 0.75-2.50%$AgNO_3$-loaded e-spun gelatin fibrous membranes, the cell viability was less than 10%. At day 10, the e-spun gelatin fibrous membranes and 0.75-1.00%Agnano-loaded e-spun gelatin fibrous membranes showed ~58%, ~52% and ~33% cell viability, respectively. For the 0.75-2.50%$AgNO_3$ and 2.50%Agnano-loaded e-spun gelatin fibrous membranes, the cell viability was less than 2%. . Representative confocal microscopy images were

assessed for monocyte adhesion and fusion for each unique sample/time point combination. Figures 6.4-6.7 (a-g) are examples of the images produced on different e-spun gelatin fibrous membrane surfaces after different culture times. Adherence was decreased with increasing time periods. This result was consistent with the cell viability from the MTT assay. With 0.75-2.50%$AgNO_3$ and 2.50%Agnano-loaded e-spun gelatin fibrous membranes, the cytoplasm (actin) of monocytes on these material surfaces did not appear on the confocal images.

For the e-spun polyester fibrous membranes, the cell viability and adherence were also seen to decrease over time. At day 0 (2h) and day 3, the cell viability and adherence showed a similar trend: PLLA > PCL ~ PBSu-DCH. At day 7, the cell viability and adherence were showed the following trend: PBSu-DCH > PLLA > PCL, and at day 10, the cell viability and adherence were as follows: PBSu-DCH > PCL > PLLA. These changes over time can be seen in Figures 6.1b and 6.2b.

The percentage of cell viability of the biodegradable polyesters; PLLA, PCL and PBSu-DCH over time can be seen in Figure 6.3b. At day 0 (2h), the cell viability of PLLA, PCL and PBSu-DCH was ~91%, ~87% and ~87%, respectively. The cell viability of PLLA, PCL and PBSu-DCH was ~71%, ~69% and ~69% at day 3, respectively. At day 7, PLLA, PCL and PBSu-DCH showed ~58, ~56 and ~59% of the cell viability, while that of PLLA, PCL and PBSu-DCH at day 10 remained at ~44%, ~45% and ~46%, Representative confocal microscopy images were assessed for monocyte adhesion and fusion for each unique sample/time point combination. Figures 6.4-6.7 (h-j) are examples of the images produced on different biodegradable polyester surfaces after different culture times. Adherence was seen to decrease over time and this result was consistent with the cell viability from the MTT assay

### 6.4.2 In vivo study

#### *6.4.2.1 Inflammatory, Wound Healing, and Fibrous Capsule Responses*

**Day 7 (week 1)**

Based on the assigned scores (Table 6.1), acute inflammation was presented for e-spun fibrous membranes of gelatin and gelatin that contained 0.75-2.50%$AgNO_3$ and 0.75-2.50%Agnano. The scores of these e-spun fibrous membranes were similar, +1, minimal. Chronic inflammation showed the following trend: 2.50%$AgNO_3$ = 2.50%Agnano > gelatin = 0.75%$AgNO_3$ = 1.00%$AgNO_3$ = 0.75%Agnano = 1.00%Agnano. Granulation tissue showed the following trend: 2.50%Agnano > 2.50%$AgNO_3$ > gelatin = 0.75%$AgNO_3$ = 1.00%$AgNO_3$ = 0.75%Agnano = 1.00%Agnano. As a result, at 7 days post-implantation, the best to worst inflammatory response was: gelatin = 0.75%$AgNO_3$ = 1.00%$AgNO_3$ = 0.75%Agnano = 1.00%Agnano > 2.50%$AgNO_3$ = 2.50%Agnano. The best to worst wound healing response was: gelatin = 0.75%$AgNO_3$ = 0.75%Agnano = 1.00%$AgNO_3$ = 1.00%Agnano > 2.50%$AgNO_3$ > 2.50%Agnano. The foreign body reaction and fibrous capsule responses of e-spun fibrous membranes of gelatin and gelatin that contained 0.75-2.50%$AgNO_3$ or 0.75-2.50%Agnano were similar. These images can be seen in Figures 6.8 (a-j) and 6.9 (a-e).

For the e-spun polyester fibrous membranes, acute inflammation was not presented (see in Table 6.1 and Figure 6.9 (e-j)) but chronic inflammation showed the same score. Granulation tissue and foreign body reaction showed the following trend: PBSu-DCH > PCL > PLLA. As a result, at 7 days post-implantation, the best to worst wound healing response was: PCL > PLLA > PBSu-DCH. However, the fibrous capsule response was similar among all materials.

**Day 14 (week 2)**

For the e-spun fibrous membranes of gelatin and gelatin that contained 0.75-2.50%$AgNO_3$ or 0.75-2.50%Agnano, acute inflammation was absent, while chronic inflammation of 1.00-2.50%$AgNO_3$ or 0.75-2.50%Agnano-containing e-spun gelatin fibrous membranes was still present (see in Figures 6.10 (a-j) and 6.11 (a-d)). The ranking of these materials based on chronic inflammation was: 2.50%Agnano > 2.50%$AgNO_3$ = 1.00%$AgNO_3$ = 0.75%Agnano > 1.00%Agnano > 0.75%$AgNO_3$. With granulation tissue and foreign body reactions, the following trend was observed: 2.50%Agnano > 0.75%Agnano > 2.50%$AgNO_3$ = 1.00%$AgNO_3$ = 1.00%Agnano > 0.75%$AgNO_3$. However, the fibrous capsule response of gelatin and gelatin that contained 0.75-2.50%$AgNO_3$ or 0.75-2.50%Agnano was similar.

Therefore, the best to worst wound healing response was: gelatin = 0.75%$AgNO_3$ > 0.75%Agnano = 1.00%Agnano > 1.00%$AgNO_3$ > 2.50%$AgNO_3$ > 2.50%Agnano.

For the e-spun polyester fibrous membranes, acute inflammation and chronic inflammation were not present, while granulation tissue and foreign body reactions showed the following trend: PLLA > PCL > PBSu-DCH. The fibrous capsule response showed a similar trend. Thus, the best to worst wound healing response was: PBSu-DCH > PCL > PLLA.

**Day 28 (week 4)**

At this time point, there was no acute or chronic inflammation for any of the materials except for the 2.50%$AgNO_3$-containing e-spun gelatin fibrous membrane. No granulation tissue was identified with any of the materials, while the foreign body reaction showed the following trend: 2.50%Agnano = 2.50%$AgNO_3$ > 1.00%$AgNO_3$ > 1.00%Agnano = 0.75%$AgNO_3$ = 0.75%Agnano = gelatin. Fibrous capsule formation showed the following trend: 1.00%Agnano > 1.00%$AgNO_3$ > 2.50%$AgNO_3$ = 2.50%Agnano = 0.75%$AgNO_3$ = 0.75%Agnano = gelatin. The best to worst wound healing response was: gelatin = 0.75%Agnano = 0.75%$AgNO_3$ > 2.50%Agnano = 2.50%$AgNO_3$ > 1.00%$AgNO_3$ = 1.00%Agnano (see in Figures 6.12 (a-j) and 6.13 (a-d)).

There was no acute or chronic inflammation for any of the polyester materials. Granulation tissue and the foreign body reaction showed the following trend: PLLA > PCL > PBSu-DCH. Fibrous capsule formation was similar. The best to worst wound healing response was: PBSu-DCH > PCL > PLLA (see in Figure 6.13 (e-j)).

## 6.5 Discussion

### 6.5.1 In vitro study

Even though silver nano-based wound dressings have received approval for clinical applications their potential dermal toxicity is reported to be a matter of concern [62]. The intended use of silver particles is also for the treatment of wounds in the form of a topical dressing. Because of their biocompatibility and biodegradability in the human body, aliphatic polyesters such as PLLA, PCL and

PBSu-DCH have attracted much attention recently in tissue engineering. Therefore, toxicity and biocompatibility evaluation (both in vitro and in vivo) of these materials is essential.

In our in vitro and in vivo studies, the known biocompatibility of gelatin is confirmed based on the temporal changes in cell adhesion and cell viability and comparison to known biocompatible materials such as silicone rubber, polyethylene terephthalate (PET), poly(L-lactic acid), polyethylene and others. To determine biocompatibility or non-biocompatibility, we have carried out statistical analysis comparing the results of each material at each time point with that of gelatin, respectively. Therefore, statistical analysis which show no statistically significant difference with gelatin, $p \geq 0.05$, is considered biocompatible and statistical analysis which show statistically significant difference, $p \leq 0.05$, compared to gelatin, is considered non-biocompatible or bioincompatible.

For the e-spun fibrous membranes of gelatin and gelatin that contained $AgNO_3$ or Agnano, at both day 0 (2h) and day 3 the cell viability and cell adhesion were shown to have the following similar trend: gelatin ~ 0.75%Agnano > 1.00%Agnano >> 0.75%$AgNO_3$ > 2.50%Agnano > 1.00%$AgNO_3$ > 2.50%$AgNO_3$ ($p < 0.0001$ statistical significance vs. gelatin except for the 0.75%Agnano e-spun fibrous membrane). At day 7 trends showed the cell viability and adherence occurring in the following rank order: gelatin ~ 0.75%Agnano > 1.00%Agnano >> 2.50%Agnano > 0.75%$AgNO_3$ ~ 1.00%$AgNO_3$ ~ 2.50%$AgNO_3$ ($p < 0.0001$ statistical significance vs. gelatin except for the 0.75%Agnano e-spun fibrous membrane), and a comparison of the 0.75-1.00%$AgNO_3$ and 1.00-2.50%$AgNO_3$-loaded e-spun fibrous membranes were statistically insignificant. At day 10 trends showed the following rank order: gelatin ~ 0.75%Agnano > 1.00%Agnano >> 0.75%$AgNO_3$ ~ 1.00%$AgNO_3$ ~ 2.50%$AgNO_3$ ~ 2.50%Agnano ($p < 0.0001$ statistical significance vs. gelatin except for the 0.75%Agnano e-spun fibrous membrane), and a comparison of the 0.75-1.00%$AgNO_3$, 1.00-2.50%$AgNO_3$ and 2.50%$AgNO_3$-2.50%Agnano-loaded e-spun fibrous membranes were statistically insignificant. These comparisons can be seen in Table 6.2 and 6.3.

Normally, it is well known that gelatin is biocompatible polymer. Based on these results, the majority of the results were statistically significantly lower when comparing the materials with e-spun gelatin fibrous membranes at each time point except for the 0.75%Agnano e-spun fibrous membrane. Cell viability and cell adhesion were greatest on the surface of e-spun gelatin fibrous membranes and then showed a marked decrease until the 10 day time point. Due to its natural gelatin protein, the presence of macrophages is identified on the surfaces of e-spun gelatin fibrous membranes at longer time points (day 7 and day 10). The cell viability and cell adhesion of the 0.75-2.50%$AgNO_3$ and 0.75-2.50%Agnano-loaded e-spun gelatin fibrous membranes were seen to significantly decrease over a period of time. These results demonstrate that silver particles have a negative, i.e. toxic, effect on monocytes. Moreover, at high silver concentrations ($AgNO_3$ or Agnano), cell viability and cell adhesion were less than at low silver concentrations at day 0 (2h) and day 3 ($p < 0.0001$ statistical significance, see in Table 6.3). While a comparison of the 0.75-250%$AgNO_3$-loaded e-spun fibrous membranes was statistically insignificant at day 7 and day 10. $AgNO_3$ had a greater effect on monocytes than Agnano at each time point ($p < 0.0001$ statistical significance, see in Table 6.3). Therefore, we demonstrated that the significant decrease of cell viability and cell adhesion was due to the effect of silver concentrations and types of silver. Additionally, from the confocal images, we demonstrated that 0.75-2.50%$AgNO_3$ and 2.50%Agnano-loaded e-spun fibrous membranes were highly toxic to monocytes because of the absence of monocyte cytoplasm.

Supporting our observation, Hidalgo et al. [63] studied the effect of $AgNO_3$ concentrations (4.1, 8.2, 16.5, 32.4, 41.2, 82.4, 164.8 and 323.7 μmol/l) at different cellular levels, the toxicity indicators of cell proliferation of human dermal fibroblasts were assessed by quantification of total protein content of the cell culture, intracellular content of ATP (the prime cellular energy donor) and DNA synthesis. They found that 8.2 μmol/l of $AgNO_3$ produces a total loss of cell protein content after 8 h of exposure. Poon et al. [64] studied the cytotoxic effects of silver on keratinocytes and fibroblasts. They demonstrated that silver is highly toxic to both keratinocytes and fibroblasts in monolayer culture and when using optimized and individualized culture the fibroblasts appear to be more sensitive to silver than

keratinocytes. Moreover, Baldi et al. [65] and Hussain et al. [66] demonstrated that silver nitrate has shown toxicity with hepatocytes and lymphocytes, respectively. Ahamed et al. [67] studied silver nanoparticle induced DNA damage and apoptosis response through the p53 pathway in mammalian cells. They found that silver nanoparticles induced p53 protein expression, DNA double strand breakage and apoptosis responses in mouse embryonic stem (mES) cells and mouse embryonic fibroblasts (MEF). However, a comparison of the 0.75%Agnano e-spun fibrous membrane with e-spun gelatin fibrous membranes was statistically insignificant at every time point. Our results suggest that the 0.75%Agnano e-spun fibrous membrane is biocompatible and the use of the Agnano material is safer than $AgNO_3$ material.

For biodegradable polyesters; PLLA, PCL and PBSu-DCH, at day 0 (2h) and day 3, the cell viability and adherence showed a similar trend: PLLA > PCL > PBSu-DCH ($p < 0.001$ statistical significance vs. PLLA at day 0 (2h)). At day 7, the cell viability and adherence showed the following trend: PBSu-DCH > PLLA > PCL, and at day 10, they were as follows: PBSu-DCH > PCL > PLLA. These comparisons of PLLA, PCL and PBSu-DCH were statistically insignificant at day 3, day 7 and day 10 that can be seen in Table 6.4. It demonstrated that these polyesters have no difference on cell viability and cell adhesion at day 3, day 7 and day 10 and all three polyesters are considered biocompatible.

Cell viability and cell adhesion cultured on the e-spun polyester fibrous membranes decreased with increasing time periods. E-spun PLLA fibrous membranes started with greater cellular viability and adhesion at day 0 (2h). However, these were the lowest by day 10 because some surface degradation had occurred and the acidic low-molecular weight degradation products and fragmented e-spun PLLA fibrous membranes [68] were lost. Sangsanoh et al. [48] investigated the in vitro responses of Schwann cells (RT4-D6P2T) on various types of e-spun fibrous scaffolds. They demonstrated that at 24h after cell seeding, these e-spun fibrous scaffolds were non-toxic to Schwann cells and the viability of the attached cells on the various substrates could be ranked as follows: PCL film > TCPS > PCL fibrous > PLLA fibrous > PHBV film > CS fibrous ~ CS film ~ PLLA film > PHB

film > PHBV fibrous > PHB fibrous. Previous reports showed that e-spun PLLA, PCL and PBSu-DCH fibrous membranes and film were also nontoxic to Schwann cells (RT4-D6P2T) [58], mouse fibroblasts (L929) [69,70], human osteoblasts (SaOS-2) [38,52], and human fibroblasts [71,72]. In this study, although the cell viability and cell adhesion were seen to decrease over a period of time, these polyesters also showed cell binding on the surface. The alignment of e-spun fibrous membranes results in greater membrane porosity that allow for cellular penetration to the inner side of the membranes. This phenomenon was observed in the confocal images. Additionally, macrophages were present on these e-spun polyester fibrous membrane surfaces at longer times (day 7 and day 10), implying the biocompatibility of these materials toward monocytes and macrophages.

6.5.2 In vivo study

In the present study we have investigated the tissue responses and in vivo biocompatibility of these e-spun fibrous membranes by comparing subcutaneous inflammation characteristics and healing response behavior to that of available materials used for tissue engineering and wound dressing applications. The analyses were separated into two materials groups, the e-spun fibrous membranes of gelatin and gelatin that contained $AgNO_3$ or Agnano and biodegradable polyesters; PLLA, PCL and PBSu-DCH.

**Day 7 (week 1)**

Chronic inflammation and the granulation tissue response were greater for 2.50%$AgNO_3$ and 2.50%Agnano at 7 days post-implantation. Foreign body reaction and fibrous capsule formation were similar among all materials. No cellular infiltration was observed for any of the materials. No surface erosion or degradation was identified for any of the materials. The effect of silver concentration was investigated and higher silver concentrations demonstrated higher chronic inflammation (see in Table 6.1). The 2.50%Agnano and 2.50%$AgNO_3$-loaded e-spun fibrous membranes showed higher chronic inflammatory responses than the other materials. Chronic inflammation most probably occurs due to high silver concentrations of silver particles. Supporting our observation, Hussain et al. [73] studied the toxicity of different sizes of silver nanoparticles on the rat liver cell line (BRL 3A) (ATCC, CRL-1442 immortalized rat liver cells). They found that after an

exposure of 24 h, the mitochondria of cells displayed abnormal size, cellular shrinkage and irregular shapes at higher concentrations of 10-50 μg/ml. Arora et al. [74] investigated that silver nanoparticle concentrations of 1.56-6.25 μg/ml were safe for the cell lines A431 (human skin carcinoma) and HT-1080 (human fibrosarcoma), but at higher concentrations of 6.25-50 μg/ml, cells became less polyhedral, shrunken and rounded. Filon et al. [75] has pointed out that silver applied as nanoparticles coated with polyvinylpirrolidone were able to permeate damaged skin in an in vitro diffusion cell system.

E-spun gelatin fibrous membranes showed the best material-tissue interface. Therefore, the overall temporal trend in the best to worst materials inflammation and wound healing responses (the biocompatibility of the implant materials) was: gelatin > 0.75%Agnano = 0.75%$AgNO_3$ = 1.00%Agnano > 1.00%$AgNO_3$ > 2.50%$AgNO_3$ = 2.50%Agnano.

In the case of polymeric biomaterials such as polyesters, the degree of tissue response such as inflammatory reaction partly depends on the chemical structure and surface hydrophilic nature of the polymer [76]. In the present study, polyesters showed minimal chronic inflammation at 7 days post-implantation, while we found that the inflammatory cell infiltration with apparent biodegradation showed the following trend: PCL > PLLA > PBSu-DCH. None of the investigated polyester materials showed any significant acute or chronic inflammation after 7 days post-implantation. The inflammatory response of surrounding tissues in the e-spun PLLA fibrous membrane at the early stage probably occurs due to the acidic low-molecular weight degradation products and fragmented e-spun fibrous membranes [68].

An important group of esterases for biodegradation of aliphatic polyester are lipases [77,78]. These enzymes are known to hydrolyze triacylglycerols (fat) to fatty acid and glycerol. The ranking of polyesters in this study based on surface erosion or degradation was: PBSu-DCH > PCL > PLLA, due to the effect of size of the nanofibers in the fibrous membranes. The average diameter of e-spun PBSu-DCH, PCL, and PLLA was 175 nm [50], 0.95 μm [38], and 1.5 μm [48], respectively. The average diameter of e-spun PBSu-DCH fibers has the smallest size, thus it has the fastest biodegradation rate. It is well known that the biodegradation rate of PCL is quite slow in film form, whereas it degrades very fast in nano- or

microparticles [79,80]. For example, a one week conventional enzymatic degradation experiment for a PCL thin film becomes a 4 min one for PCL nanoparticles [80].

The foreign body reaction showed the following trend: PBSu-DCH > PCL > PLLA, with a single monolayer of macrophages and foreign body giant cells present at the interface between the material and the tissue. The form and topography of the surface of the biomaterial determine the compositions of the foreign body reaction. With biocompatible materials, composition of the foreign body reaction in the implant site may be controlled by the surface properties of the biomaterial, form of the implant, and relationship between the surface area of the biomaterial and volume of the implant [5]. For example, fabrics, porous materials, particulate, or microspheres will have higher densities of macrophages and foreign body giant cells in the implant site than smooth-surface implants due to high-surface-to-volume implants.

Therefore, the overall temporal trend in the best to worst biocompatible materials was: PLLA = PCL = PBSu-DCH.

**Day 14 (week 2)**

Chronic inflammation showed the following trend: 2.50%Agnano > 2.50%$AgNO_3$ = 1.00%$AgNO_3$ = 0.75%Agnano > 1.00%Agnano > 0.75%$AgNO_3$ = gelatin. Normally, acute and chronic inflammation should be absent after 7 days post-implantation, whereas they still occurred due to the presence of a long-standing infection such as silver. High silver concentrations cause damage to cells. Granulation tissue response showed the following trend: 2.50%Agnano > 2.50%$AgNO_3$ = 1.00%$AgNO_3$ > 0.75%$AgNO_3$ = 1.00%Agnano = 0.75%Agnano = gelatin.

$AgNO_3$ materials had a greater effect on inflammation and wound healing responses than Agnano materials (see in Table 6.1) and $AgNO_3$ materials also showed higher foreign body reactions at the material/tissue interface than the Agnano materials because of the toxicity of nitrate. Supporting our observation, Atiyeh et al. [81] reported that nitrate is toxic to wounds and to cells and appears to decrease healing, offsetting to some degree the beneficial antibacterial effect of silver. Moreover, the reduction of nitrate to nitrite causes oxidant induced cell

damage. Foley et al. [82] and Li et al. [83] showed that nanosized particles of various chemistries can damage mitochondria of cells.

Some degradation was present at the e-spun fibrous membrane surfaces after 14 days post-implantation and showed the following trend: gelatin > 0.75%$AgNO_3$ > 0.75%Agnano = 1.00%$AgNO_3$ = 1.00%Agnano > 2.50%$AgNO_3$ = 2.50%Agnano. E-spun gelatin demonstrated the highest degradation rate and cells can easily proliferate at the material surface. Foreign body reaction showed the following trend: 2.50%Agnano = 2.50%$AgNO_3$ = 1.00%$AgNO_3$ = 1.00%Agnano = 0.75%Agnano > 0.75%$AgNO_3$ = gelatin. Fibrous capsule formation was similar among all materials. Therefore, the overall temporal trend in the best to worst biocompatible materials was: gelatin = 0.75%Agnano = 0.75%$AgNO_3$ = 1.00%Agnano > 1.00%$AgNO_3$ > 2.50%$AgNO_3$ = 2.50%Agnano.

For polyesters, none of the investigated materials showed any significant acute or chronic inflammation after 14 days post-implantation, while cell infiltration showed the following trend: PLLA > PCL > PBSu-DCH. Degradation of these polyesters due to the effect of fibrous diameter showed the following trend: PBSu-DCH > PCL > PLLA. The foreign body reaction showed the following trend: PBSu-DCH > PLLA > PCL. The overall temporal trend in the best to worst biocompatible materials was: PBSu-DCH = PCL > PLLA.

**Day 28 (week 4)**

There was no acute or chronic inflammation for any of the materials except for the 2.50%$AgNO_3$-containing e-spun gelatin fibrous membranes after 28 days post-implantation, which was identified due to the effect of silver concentration and the toxicity of nitrate. The foreign body reaction showed the following trend: 2.50%Agnano = 2.50%$AgNO_3$ = 1.00%$AgNO_3$ > 1.00%Agnano = 0.75%$AgNO_3$ = 0.75%Agnano = gelatin. Therefore, the overall temporal trend in the best to worst biocompatible materials was: gelatin = 0.75%Agnano = 0.75%$AgNO_3$ = 1.00%Agnano > 1.00%$AgNO_3$ > 2.50%$AgNO_3$ = 2.50%Agnano.

None of the polyesters demonstrated any acute or chronic inflammation after 28 days post-implantation, while degradation showed the following trend: PBSu-DCH > PCL > PLLA. The foreign body reaction showed the following trend: PBSu-

DCH = PLLA = PCL. The overall trend in the best to worst biocompatible materials was: PBSu-DCH = PCL = PLLA.

From these results, we can conclude that some surface erosion or degradation occurred with the e-spun fibrous membranes of gelatin and gelatin that contained $AgNO_3$ or Agnano and showed the overall trend: gelatin > 0.75%Agnano = 0.75%$AgNO_3$ = 1.00%Agnano > 1.00%$AgNO_3$ > 2.50%$AgNO_3$ = 2.50%Agnano. Foreign body reaction at the surface of these materials presented the overall trend: 2.50%Agnano = 2.50%$AgNO_3$ = 1.00%$AgNO_3$ > 1.00%Agnano = 0.75%$AgNO_3$ = 0.75%Agnano = gelatin. Moreover, the overall biocompatibility of the materials showed the following trend: gelatin = 0.75%Agnano = 0.75%$AgNO_3$ > 1.00%Agnano > 1.00%$AgNO_3$ > 2.50%$AgNO_3$ > 2.50%Agnano.

For polyesters materials, surface erosion or degradation showed the overall trend: PBSu-DCH > PCL > PLLA, and the foreign body reaction at the surface showed the overall trend: PBSu-DCH = PCL > PLLA. The overall biocompatibility polyester materials are represented as: PBSu-DCH = PCL = PLLA.

## 6.6 Conclusion

In the present paper we report on both in vitro and in vivo biocompatibility studies of e-spun fibrous membranes of gelatin and gelatin that contained 0.75-2.50% w/w (based on the weight of the gelatin powder) $AgNO_3$ or Agnano, and biodegradable polyesters; PLLA, PCL and PBSu-DCH. In vitro responses of monocytes/macrophages on various types of e-spun fibrous membranes were evaluated at each time point (day 0 (2h), 3, 7 and 10). Statistical analysis was conducted comparing cell viability and cell adhesion on each test material at each time point compared to the control e-spun gelatin fibrous membranes. Cell viability and cell adhesion were greatest on the surface of e-spun gelatin fibrous membranes and showed an expected decrease over the 10 day time period. A comparison of the 0.75%Agnano e-spun fibrous membrane with e-spun gelatin fibrous membranes was statistically insignificant at each time point ($p > 0.05$) demonstrating biocompatibility. The cell viability and cell adhesion of the 0.75-2.50%$AgNO_3$ and 1.00-2.50%Agnano-loaded e-spun gelatin fibrous membranes were significantly

lower when compared to the e-spun gelatin fibrous membranes demonstrating bioincompatibility or toxicity. Materials with high concentrations of $AgNO_3$ displayed lower cell viability and adhesion than materials with low concentrations of $AgNO_3$ at day 0 (2h) and 3, while these comparisons were statistically insignificant at day 7 and day 10. High Agnano concentrations resulted in reduced cell viability and adhesion when compared to low concentrations of Agnano at each time point. At the same concentration (i.e., 0.75%$AgNO_3$-075%Agnano, 1.00%$AgNO_3$-1.00%Agnano, 2.50%$AgNO_3$-2.50%Agnano), $AgNO_3$ had a greater negative effect on cell viability and adhesion, i.e. toxicity, than Agnano at each time point, except for the 2.50%$AgNO_3$-2.50%Agnano at day 10, it was statistically insignificant . Therefore, we conclude that the 0.75-2.50%$AgNO_3$ and 1.00-2.50%Agnano-loaded e-spun fibrous membranes were toxic to monocytes/macrophages, whereas the 0.75%Agnano-loaded e-spun fibrous membrane is as biocompatible as e-spun gelatin fibrous membranes.

In the in vivo study, e-spun gelatin fibrous membranes showed the best biocompatibility. Higher silver concentrations caused higher chronic inflammation and $AgNO_3$ material caused increased inflammation and wound healing responses compare to Agnano materials. Therefore, we conclude that high concentrations of silver particles can cause damage to cells. Nitrate is also shown to be toxic to cells and appears to reduce the healing response. Results from the in vivo studies were comparable to those from the in vitro studies with the e-spun gelatin fibrous membranes and the 0.75%Agnano demonstrating the earliest rapid resolution of the acute and chronic inflammatory responses with mild foreign body reactions and mild to moderate fibrous capsule formation at 14 and 28 days.

For the in vitro cell viability and adhesion of e-spun PLLA, PCL and PBSu-DCH fibrous membranes results showed that these polyesters were statistically comparable and biocompatible. In the in vivo study, these polyester materials demonstrated biocompatibility with normal expected and comparable inflammatory, foreign body reaction, and wound healing responses.

## 6.7 Acknowledgments

The authors acknowledge partial support received from Dr. Anderson's laboratory; Department of Pathology at Case Western Reserve University (Cleveland, Ohio, USA), the National Nanotechnology Center (grant number: BR0108); the National Center of Excellence for Petroleum, Petrochemicals, and Advanced Materials (NCE-PPAM); and the Petroleum and Petrochemical College (PPC), Chulalongkorn University. PR acknowledges a doctoral scholarship received from the Thailand Graduate Institute of Science and Technology (TGIST) (TG-55-09-49-067D).

## 6.8 References

[1] Anderson JM. Biological responses to materials. Annu Rev Mater Res 2001;31:81-110.

[2] Anderson JM, Rodriguez A, Chang DT. Foreign body reaction to biomaterials. Semin Immunol 2008;20(2):86-100.

[3] Brodbeck WG, Shive MS, Colton E, Nakayama Y, Matsuda T, Anderson JM. Influence of biomaterials surface chemistry on apoptosis of adherent cells. J Biomed Mater Res 2001;55: 661-668.

[4] Brodbeck WG, Nakayama Y, Matsuda T, Colton E, Ziats NP, Anderson JM. Biomaterial surface chemistry dictates adherent monocyte/macrophage cytokine expression in vitro. CYTOKINE 2002;18(6):311–319

[5] Anderson JM, Cook G, Costerton B, Hanson SR, Hensten-Pettersen A, Jacobsen N, Johnson RJ, Mitchell RN, Pasmore M, Schoen FJ, Shirtliff M, Stoodley P. Biomaterial Science, 2nd edition: Host Reactions to Biomaterials and Their Evaluation. San Diego: Elsevier Academic Press Inc., 2004;293-304 [chapter 4].

[6] McNally AK, Anderson JM. Interleukin-4 induces foreign body giant cells from human monocytes/macrophages. Differential lymphokine regulation of macrophage fusion leads to morphological variants of multinucleated giant cells. Am. J. Pathol. 1995;147:1487–1499.

[7] McNally AK. Foreign body-type multinucleated giant cell formation requires protein kinase C β, δ and ζ, Experimental and Molecular Pathology 2008;84:37-45.

[8] Zhao Q, Topham N, Anderson JM, Lodoen G, Payet CR. Foreign-body giant cells and polyurethane biostaility: in vivo correlation of cell adhesion and surface cracking. J Biomed Mater Res 1991;25(2):177-183.

[9] Zhao QH, McNally AK, Rubin KR, Renier M, Wu Y, Rose-Caprara V, Anderson JM, Hiltner A, Urbanski P, Stokes K. Human plasma alpha 2-macroglobulin promotes in vitro oxidative stress cracking of Pellethane 2363-80A: in vivo and in vitro correlations. J Biomed Mater Res 1993;27(3):379-388.

[10] Eskin S, Horbett T, McIntire L, Nitchell R, Ratner B, Schoen F, Yee A. Some Background Concepts. In: Ratner BD, Hoffman, A.S., Schoen, F.J., Lemons, J.E., editors. Biomaterial Science: An Introduction to Materials in Medicine. San Diego: Elsevier Academic Press Inc., 2004;p237-291.

[11] Wilson CJ, Clegg RE, Leavesley DI, Pearcy MJ. Mediation of biomaterial-cell interactions by absorbed proteins: review. Tissue Eng 2005;28(22):3272-3283.

[12] Reneker DH, Yarin AL. Electrospinning jets and polymer nanofibers. Polymer 2008;49:2387–425.

[13] Schreuder-Gibson HL, Gibson P, Tsai P, Gupta P, Wilkes G. Cooperative charging effects of fibers from electrospinning of electrically dissimilar polymers. International Nonwovens Journal 2004;13:39–45.

[14] Schreuder-Gibson H, Gibson P, Wadsworth L, Hemphill S, Vontorcik J. Effect of filter deformation on the filtration and air flow for elastomeric nonwoven media. Advances in Filtration and Separation Technology 2002;15:525–537.

[15] Gibson P, Schreuder-Gibson H, Rivin D. Transport properties of porous membranes based on electrospun nanofibers. Colloids and Surfaces. A Physicochemical and Engineering Aspects 187188 2001;469–481.

[16] Wannatong L, Sirivat A. Electrospun fibers of polypyrrole/polystyrene blend for gas sensing applications. PMSE Preprints 2004;91:692–693.

[17] Wang XY, Kim YG, Drew C, Ku BC, Kumar J, Samuelson LA. Electrostatic assembly of conjugated polymer thin layers on electrospun nanofibrous membranes for biosensors. Nano Letters 2004;4:331–334.

[18] Ding B, Kim J, Fujimoto K, Shiratori S. Electrospun nanofibrous polyelectrolyte membranes for advanced chemical sensors. Chemical Sensors 2004;20:264–265.

[19] Kim C, Park SH, Lee WJ, Yang KS. Characteristics of supercapacitor electrodes of PBI-based carbon nanofiber web prepared by electrospinning. Electrochimica Acta 2004;50:877–881.

[20] Kim C, Choi YO, Lee WJ, Yang KS. Supercapacitor performances of activated carbon fiber webs prepared by electrospinning of PMDA-ODA poly(amic acid) solutions. Electrochimica Acta 2004;50:883–887.

[21] Kim C, Yang KS, Lee WJ. The use of carbon nanofiber electrodes prepared by electrospinning for electrochemical supercapacitors, Electrochemical and Solid-State Letters 2004;7:A397–A399.

[22] Liang D, Hsiao B, Chu B. Functional electrospun nanofibrous scaffolds for biomedical application. Advanced Drug Delivery Reviews 2007;59:1392-1412.

[23] Agarwal S, Wendroff J, Greiner A. Use of electrospinning technique for biomedical applications. Polymer 2008;49:5603-5621.

[24] Sill TJ, von Recum HA. Electrospinning: Applications in drug delivery and tissue engineering. Biomaterials 2008;29:1989-2006.

[25] Wu LL, Yuan XY, Sheng J. Immobilization of cellulase in nanofibrous PVA membranes by electrospinning. J Membr Sci 2005;250:167–173.

[26] Choi JS, Lee SW, Jeong L, Bae SH, Min BC, Youk JH. Effect of organosoluble salts on the nanofibrous structure of electrospun poly(3-hydroxybutyrate-co-3-hydroxyvalerate). Int J Biol Macromol 2004;34:249–256.

[27] Kim K, Luu YK, Chang C, Fang DF, Hsiao BS, Chu B. Incorporation and controlled release of a hydrophilic antibiotic using poly(lactide-co-glycolide)-based electrospun nanofibrous scaffolds. J Controlled Release 2004;98:47–56.

[28] Rujitanaroj P, Pimpha N, Supaphol P. Wound-dressing materials with antibacterial activity from electrospun gelatin fiber mats containing silver nanoparticles. Polymer 2008;49:4723–4732

[29] Hong KH. Preparation and properties of electrospun poly(vinyl alcohol)/silver fiber web as wound dressings. Polym Eng Sci 2007;47:43–49.

[30] Khil MS, Cha DI, Kim HY, Kim I,S Bhattarai N. Electrospun nanofibrous polyurethane membrane as wound dressing, Journal of Biomedical Materials Research. Part B, Applied Biomaterials 2003;67B:675–679.

[31] Kim HY, Lee BM, Kim IS, Jin TH, Ko KH, Ryu YJ. Fabrication of triblock copolymer of poly(r-dioxanone-co-L-lactide)-block-poly(ethylene glycol) nonwoven mats by electrospinning and applications for wound dressing. PMSE Preprints 2004;91:712–713.

[32] Luu YK, Kim K, Hsiao BS, Chu B, Hadjiargyrou M. Development of a nanostructured DNA delivery scaffold via electrospinning of PLGA and PLA–PEG block copolymers. J Controlled Release 2003;89:341–353.

[33] Kenawy ER, Bowlin GL, Mansfield K, Layman J, Simpson DG, Sanders EH. Release of tetracycline hydrochloride from electrospun poly(ethylene-covinylacetate), poly(lactic acid), and a blend. J Controlled Release 2002;81:57–64.

[34] Zeng J, Xu X, Chen X, Liang Q, Bian X, Yang L. Biodegradable electrospun fibers for drug delivery. J Controlled Release 2003;92:227–231.

[35] Verreck G, Chun I, Rosenblatt J, Peeters J, van Dijck A, Mensch J. Incorporation of drugs in an amorphous state into electrospun nanofibers composed of a water-insoluble, nonbiodegradable polymer. J Controlled Release 2003;92;349–360.

[36] Young S, Wong M, Tabata Y, Mikos AG. Gelatin as a delivery vehicle for the controlled release of bioactive molecules. J Controlled Release 2005;109:256–274.

[37] Lannutti J, Reneker D, Ma T, Tomasko D, Farson D. Electrospinning for tissue engineering scaffolds. Materials Science and Engineering C 2007;27:504–509.

[38] Wutticharoenmongkol P, Sanchavanakit N, Pavasan P, Supaphol P. Novel Bone Scaffolds of Electrospun Polycaprolactone Fibers. Journal of Nanoscience and Nanotechnology 2006;6: 514–522.

[39] Meechaisue C, Dubin R, Supaphol P, Hoven VP, Kohn J. Electrospun mat of tyrosine-derived polycarbonate fibers for potential use as tissue scaffolding material. J Biomater Sci Polym Ed 2006;17(9):1039-1056.

[40] Zhang YZ, Venugopal J, Huang ZM, Lim CT, Ramakrishna S. Characterization of the surface biocompatibility of the electrospun PCL-collagen nanofibers using fibroblasts. Biomacromolecules 2005;Sep-Oct;6(5):2583-2589.

[41] Dalton PD, Lleixa Calvet J, Mourran A, Klee D, Moller M. Melt electrospinning of poly-(ethylene glycol-block-epsilon-caprolactone). Biotechnol J 2006;Sep;1(9):998-1006.

[42] Thomas V, Jose MV, Chowdhury S, Sullivan JF, Dean DR, Vohra YK. Mechano-morphological studies of aligned nanofibrous scaffolds of polycaprolactone fabricated by electrospinning. J Biomater Sci Polym Ed 2006;17(9):969-984.

[43] Kim K, Yu M, Zong X, Chiu J, Fang D, Seo YS. Control of degradation rate and hydrophilicity in electrospun non-woven poly(D,L-lactide) nanofiber scaffolds for biomedical applications. Biomaterials 2003;Dec;24(27):4977-4985.

[44] Yang F, Murugan R, Wang S, Ramakrishna S. Electrospinning of nano/microscale poly(L-lactic acid) aligned fibers and their potential in neural tissue engineering. Biomaterials 2005;May;26(15):2603-2610.

[45] Cui W, Li X, Zhou S, Weng J. In situ growth of hydroxyapatite within electrospun poly(DL-lactide) fibers. J Biomed Mater Res A 2007;Sep;15;82(4):831-841.

[46] Kim TG, Park TG. Biomimicking extracellular matrix: cell adhesive RGD peptide modified electrospun poly(D,L-lactic-co-glycolic acid) nanofiber mesh. Tissue Eng 2006;Feb;12(2):221-233.

[47] Park KE, Kang HK, Lee SJ, Min BM, Park WH. Biomimetic nanofibrous scaffolds: preparation and characterization of PGA/chitin blend nanofibers. Biomacromolecules 2006;Feb;7(2):635-643.

[48] Sangsanoh P, Waleetorncheepsawat S, Suwantong O, Wutticharoenmongkol P, Weeranantanapan O, Chuenjitbuntaworn B, Cheepsunthorn P, Pavasant P, Supaphol P. In Vitro Biocompatibility of Schwann Cells on Surfaces of Biocompatible Polymeric Electrospun Fibrous and Solution-Cast Film Scaffolds. Biomacromolecules 2007;8:1587-1594.

[49] Meng W, Kim SY, Yuan J, Kim JC, Kwon OH, Kawazoe N. Electrospun PHBV/collagen composite nanofibrous scaffolds for tissue engineering. J Biomater Sci Polym Ed 2007;18(1):81-94.

[50] Sutthiphong S, Pavasant P, Supaphol P. Electrospun 1,6-diisocyanatohexane-extended poly(1,4-butylene succinate) fiber mats and their potential for use as bone scaffolds. Polymer *2009*;50(6):1558-1568.

[51] Kenawy R, Layman JM, Watkins JR, Bowlin GL, Matthews JA, Simpson DG, Wnek GE. Electrospinning of poly(ethylene-co-vinyl alcohol) fibers. Biomaterials 2003;24:907–913.

[52] Rho KS, Jeong L, Lee G, Seo BM, Park YJ, Hong SD, Roh S, Cho JJ, Park WH, Min BM. Electrospinning of collagen nanofibers: effects on the behavior of normal human keratinocytes and early-stage wound healing. Biomaterials 2006;27:1452–1461.

[53] Casper CL, Yang W, Farach-Carson MC, Rabolt JF. Coating electrospun collagen and gelatin fibers with perlecan domain I for increased growth factor binding. Biomacromolecules 2007; Apr;8(4):1116-1123.

[54] Khil MS, Cha DI, Kim HY, Kim IS, Bhattarai N. Electrospun nanofibrous polyurethane membrane as wound dressing. J Biomed Mater Res B Appl Biomater 2003;67:675–679.

[55] Muzzarelli RAA. Chitins and chitosans for the repair of wounded skin, nerve, cartilage and bone. Carbohydrate Polymers 2009;76:167–182.

[56] Suwantong O, Ruktanonchai U, Supaphol P. Electrospun cellulose acetate fiber mats containing asiaticoside or Centella asiatica crude extract and the release characteristics of asiaticoside. Polymer 2008;49:4239–4247.

[57] Veparia C, Kaplan DL. Silk as a biomaterial. Prog Polym Sci 2007;32:991–1007.

[58] He S, Yao J, Jiang P, Shi D, Zhang H, Xie S, Pang S,Gao H. Formation of Silver Nanoparticles and Self-Assembled Two-Dimensional Ordered Superlattice. *Langmuir* 2001;*17:*1571-1575.

[59] Xu X, Yang Q, Wang Y, Yu H. Biodegradable electrospun poly(L-lactide) fibers containing antibacterial silver nanoparticles. European Polymer Journal 2006;42:2081-2087.

[60] Voskerician G, Shive MS, Shawgo RS, Recum HV, Anderson JM, Cima MJ, Langer R. Biocompatibility and biofouling of MEMS drug delivery devices. Biomaterials 2003;24:1959-1967.

[61] Voskerician G, Gingras PH, Anderson JM. Macroporous condensed poly(tetrafluoroethylene). I. In vivo inflammatory response and healing characteristics. J Biomed Mater. Res. Part A. 2005;76A(2):234-242.

[62] Chen X, Schluesener HJ. Nanosilver: a nanoproduct in medical application. Toxicol Lett 2008;176:1–12.

[63] Hidalgo E, Domínguez C. Study of cytotoxicity mechanisms of silver nitrate in human dermal fibroblasts. Toxicology Letters 1998;98:169–179.

[64] Poon VKM, Burd A. In vitro cytotoxity of silver: implication for clinical wound care. Burns 2004;30:140–147.

[65] Baldi C, Minoia C, Di Nuici A, Capodaglio E, Manzo L, Effects of silver in isolated rat hepatocytes. Toxicol Lett 1988;41:261-68.

[66] Hussain S, Anner RM, Anner BM, Cysteine protects Na, K-ATPase and isolated human lymphocytes from silver toxicity. Biochem Biophys Res Commun 1992;189:1444-49.

[67] Ahamed M, Karns M, Goodson M, Rowe J, Hussain SM, Schlager JJ, Hong Y. DNA damage response to different surface chemistry of silver nanoparticles in mammalian cells. Toxicology and Applied Pharmacology 2008;233:404–410.

[68] Ishii D, Ying TH, Mahara A, Murakami S, Yamaoka T, Lee W, Iwata T. In Vivo Tissue Response and Degradation Behavior of PLLA and Stereocomplexed PLA Nanofibers. Biomacromolecules 2009;10(2):237-242.

[69] Wang YQ, Cai JY. Enhanced cell affinity of poly(L-lactic acid) modified by base hydrolysis: Wettability and surface roughness at nanometer scale. Current Applied Physics 2007;7S1:e108–e111.

[70] Serranoa MC, Pagania R, Vallet-Regí M, Peña J, Ràmila A, Izquierdob I.,. Portolés MT. In vitro biocompatibility assessment of poly(e-caprolactone) films using L929 mouse fibroblasts. Biomaterials 2004;25:5603–5611.

[71] Doyle V, Pearson R, Lee D, Wolowacz S, McTaggart S. An investigation of the growth of human dermal fibroblasts on poly-L-lactic acid in vitro. Journal of Materials Science: Materials In Medicine 1996;71:381-385.

[72] Venugopal JR, Zhang Y, Ramakrishna S. In Vitro Culture of Human Dermal Fibroblasts on Electrospun Polycaprolactone Collagen Nanofibrous Membrane. Artificial Organs and Transplantation 2006;30(6):440–446.

[73] Hussain S, Hess K, Gearhart J, Geiss K, Schlager J. In vitro toxicity of nanoparticles in BRL3A rat liver cells. Toxicol In vitro 2005;19:975–83.

[74] Arora S, Jain J, Rajwade JM, Paknikar KM. Cellular responses induced by silver nanoparticles: In vitro studies. Toxicol. Lett. 2008;179:93–100.

[75] Filon FL, D'Agostin F, Crosera M, Adami G, Renzi N, Bovenzi M, Maina G. Human skin penetration of silver nanoparticles through intact damaged skin. Toxicology 2009;255:33–37.

[76] Wang YX, Robertson JL, Spillman WB, Claus RO. Effects of the Chemical Structure and the Surface Properties of Polymeric Biomaterials on Their Biocompatibility. Pharm. Res. 2004;21:1362-1373.

[77] Tokiwa Y, Suzuki T, Takeda K. Two Types of Lipases in Hydrolysis of Polyester. Agric. Biol. Chem. 1988;52(8),1943-1988.

[78] Tokiwa Y, Calabia BP. Biodegradability and biodegradation of poly(lactide). Appl Microbiol Biotechnol 2006;72:244–251.

[79] Gan H, Fung JT, Jing XB, Wu C, Kuliche WK. A novel laser light-scattering study of enzymatic biodegradation of poly(ε-caprolactone) nanoparticles. Polymer 1999;40:1961-1967.

[80] Wu C, Gan Z. A novel method of studying polymer biodegradation. Polymer 1998;39: 4429-4431.

[81] Atiyeh BS, Costagliola M, Hayek SN, Dibo SA. Effect of silver on burn wound infection control and healing: Review of the literature. Burns 2007;33:139–148.

[82] Foley S, Crowley C, Smaihi M, Bonfils C, Erlanger BF, Seta P. Cellular localization of a water-soluble fullerene derivative. Biochem. Biophys. Res. Commun. 2002;294:116–119.

[83] Li N, Sioutas C, Cho A, Schmitz D, Misra C, Sempf J. Ultrafine particulate pollutants induce oxidative stress and mitochondrial damage. Environ. Health Perspect. 2003;111:455–460.

**Table 6.1** Scoring system on all phases of the inflammatory and wound healing response and fibrous capsule structure response (week 1, 2 and 4)

| Implant Materials | Acute Inflammation | Chronic Inflammation | Granulation Tissue | Foreign Body Reaction (FBR) | Fibrous Capsule |
|---|---|---|---|---|---|
| e-spun gelatin | +1 | +1 | +1 | +1 | +1 |
| 0.75%$AgNO_3$ | +1 | +1 | +1 | +1 | +1 |
| 1.00%$AgNO_3$ | +1 | +1 | +1 | +1 | +1 |
| 2.50%$AgNO_3$ | +1 | +2 | +2 | +1 | +1 |
| 0.75%Agnano | +1 | +1 | +1 | +1 | +1 |
| 1.00%Agnano | +1 | +1 | +1 | +1 | +1 |
| 2.50%Agnano | +1 | +2 | +3 | +1 | +1 |
| e-spun PLLA | 0 | +1 | +1 | +2 | +1 |
| e-spun PCL | 0 | +1 | +1 | +2 | +1 |
| e-spun PBSu | 0 | +1 | +1 | +3 | +1 |

| Implant Materials | Acute Inflammation | Chronic Inflammation | Granulation Tissue | Foreign Body Reaction (FBR) | Fibrous Capsule |
|---|---|---|---|---|---|
| e-spun gelatin | 0 | 0 | 0 | +1 | +2 |
| 0.75%$AgNO_3$ | 0 | 0 | 0 | +1 | +2 |
| 1.00%$AgNO_3$ | 0 | 1.5 | 1.5 | +2 | +2 |
| 2.50%$AgNO_3$ | 0 | 1.5 | 1.5 | +2 | +2 |
| 0.75%Agnano | 0 | 1.5 | +2 | +2 | +2 |
| 1.00%Agnano | 0 | +1 | +1 | +2 | +2 |
| 2.50%Agnano | 0 | +2 | 2.5 | +2 | +2 |
| e-spun PLLA | 0 | 0 | +3 | +4 | +3 |
| e-spun PCL | 0 | 0 | +1 | +3 | +2 |
| e-spun PBSu | 0 | 0 | 0 | +2 | +2 |

| Implant Materials | Acute Inflammation | Chronic Inflammation | Granulation Tissue | Foreign Body Reaction (FBR) | Fibrous Capsule |
|---|---|---|---|---|---|
| e-spun gelatin | 0 | 0 | 0 | +2 | +2 |
| 0.75%$AgNO_3$ | 0 | 0 | 0 | +2 | +2 |
| 1.00%$AgNO_3$ | 0 | 0 | 0 | 2.5 | +3 |
| 2.50%$AgNO_3$ | 0 | 1.5 | 0 | 2.5 | 2.5 |
| 0.75%Agnano | 0 | 0 | 0 | +2 | +2 |
| 1.00%Agnano | 0 | 0 | 0 | +2 | 3.5 |
| 2.50%Agnano | 0 | 0 | 0 | +2.5 | +2 |
| e-spun PLLA | 0 | 0 | +3 | +4 | +3 |
| e-spun PCL | 0 | 0 | +1 | +4 | +3 |
| e-spun PBSu | 0 | 0 | 0 | +4 | +3 |

**Score: 0 = none; 1 = minimal; 2 = mild; 3 = moderate; and 4 = extensive**

**Table 6.2** *P* values of comparison between e-spun gelatin fibrous membranes and 0.75-2.50%$AgNO_3$ and 0.75-2.50%Agnano-loaded e-spun gelatin fibrous membranes on cell viability and cell adhesion

| **(a)** | **Cell viability from the MTT assay** | | | |
|---|---|---|---|---|
| **Materials** | **Comparison to Gelatin, *P* value** | | | |
| | **Day 0 (2h)** | **Day 3** | **Day 7** | **Day 10** |
| 0.75%$AgNO_3$ | 0.0001 | 0.0001 | 0.0001 | 0.0001 |
| 1.00%$AgNO_3$ | 0.0001 | 0.0001 | 0.0001 | 0.0001 |
| 2.50%$AgNO_3$ | 0.0001 | 0.0001 | 0.0001 | 0.0001 |
| 0.75%Agnano | 0.120* | 0.072* | 0.063* | 0.052* |
| 1.00%Agnano | 0.0001 | 0.0001 | 0.0001 | 0.0001 |
| 2.50%Agnano | 0.0001 | 0.0001 | 0.0001 | 0.0001 |

| **(b)** | **Cell adhesion from Confocal microscopy** | | | |
|---|---|---|---|---|
| **Materials** | **Comparison to Gelatin, *P* value** | | | |
| | **Day 0 (2h)** | **Day 3** | **Day 7** | **Day 10** |
| 0.75%$AgNO_3$ | 0.0001 | 0.0001 | 0.0001 | 0.0001 |
| 1.00%$AgNO_3$ | 0.0001 | 0.0001 | 0.0001 | 0.0001 |
| 2.50%$AgNO_3$ | 0.0001 | 0.0001 | 0.0001 | 0.0001 |
| 0.75%Agnano | 0.210* | 0.084* | 0.059* | 0.054* |
| 1.00%Agnano | 0.0001 | 0.0001 | 0.0001 | 0.0001 |
| 2.50%Agnano | 0.0001 | 0.0001 | 0.0001 | 0.0001 |

*Considered biocompatible when compared to e-spun gelatin fibrous membranes

**Table 6.3** *P* values of comparison between silver concentrations and types of silver of on cell viability and cell adhesion

| (a) Cell viability from the MTT assay | | | | |
|---|---|---|---|---|
| **Materials** | ***P* value** | | | |
| | **Day 0 (2h)** | **Day 3** | **Day 7** | **Day 10** |
| 0.75%$AgNO_3$-1.00%$AgNO_3$ | 0.0001 | 0.001 | 0.067 | 0.87 |
| 1.00%$AgNO_3$-2.50%$AgNO_3$ | 0.0001 | 0.001 | 0.082 | 0.35 |
| 0.75%Agnano-1.00%Agnano | 0.003 | 0.005 | 0.002 | 0.001 |
| 1.00%Agnano-2.50%Agnano | 0.001 | 0.0001 | 0.0001 | 0.0001 |
| 0.75%$AgNO_3$-0.75%Agnano | 0.001 | 0.0001 | 0.0001 | 0.0001 |
| 1.00%$AgNO_3$-1.00%Agnano | 0.001 | 0.0001 | 0.0001 | 0.0001 |
| 2.50%$AgNO_3$-2.50%Agnano | 0.0001 | 0.0001 | 0.0001 | 0.078 |

| (b) Cell adhesion from Confocal microscopy | | | | |
|---|---|---|---|---|
| **Materials** | ***P* value** | | | |
| | **Day 0 (2h)** | **Day 3** | **Day 7** | **Day 10** |
| 0.75%$AgNO_3$-1.00%$AgNO_3$ | 0.0001 | 0.001 | 0.056 | 0.18 |
| 1.00%$AgNO_3$-2.50%$AgNO_3$ | 0.0001 | 0.001 | 0.064 | 0.27 |
| 0.75%Agnano-1.00%Agnano | 0.001 | 0.0001 | 0.0001 | 0.0001 |
| 1.00%Agnano-2.50%Agnano | 0.001 | 0.0001 | 0.0001 | 0.0001 |
| 0.75%$AgNO_3$-0.75%Agnano | 0.0001 | 0.0001 | 0.0001 | 0.0001 |
| 1.00%$AgNO_3$-1.00%Agnano | 0.0001 | 0.0001 | 0.0001 | 0.0001 |
| 2.50%$AgNO_3$-2.50%Agnano | 0.0001 | 0.0001 | 0.0001 | 0.053 |

**Table 6.4** *P* values of comparison to biodegradable polyesters; PLLA, PCL and PBSu-DCH on cell viability and cell adhesion

| **Cell viability from the MTT assay** | | | | |
|---|---|---|---|---|
| **Materials** | ***P* value** | | | |
| | **Day 0 (2h)** | **Day 3** | **Day 7** | **Day 10** |
| PLLA-PCL | 0.013 | 0.17 | 0.073 | 0.20 |
| PLLA-PBSu | 0.0063 | 0.17 | 0.059 | 0.053 |
| PCL-PBSu | 0.091 | 0.092 | 0.068 | 0.250 |
| **Cell adhesion from Confocal microscopy** | | | | |
| PLLA-PCL | 0.001 | 0.062 | 0.40 | 0.054 |
| PLLA-PBSu | 0.003 | 0.058 | 0.27 | 0.063 |
| PCL-PBSu | 0.074 | 0.081 | 0.052 | 0.055 |

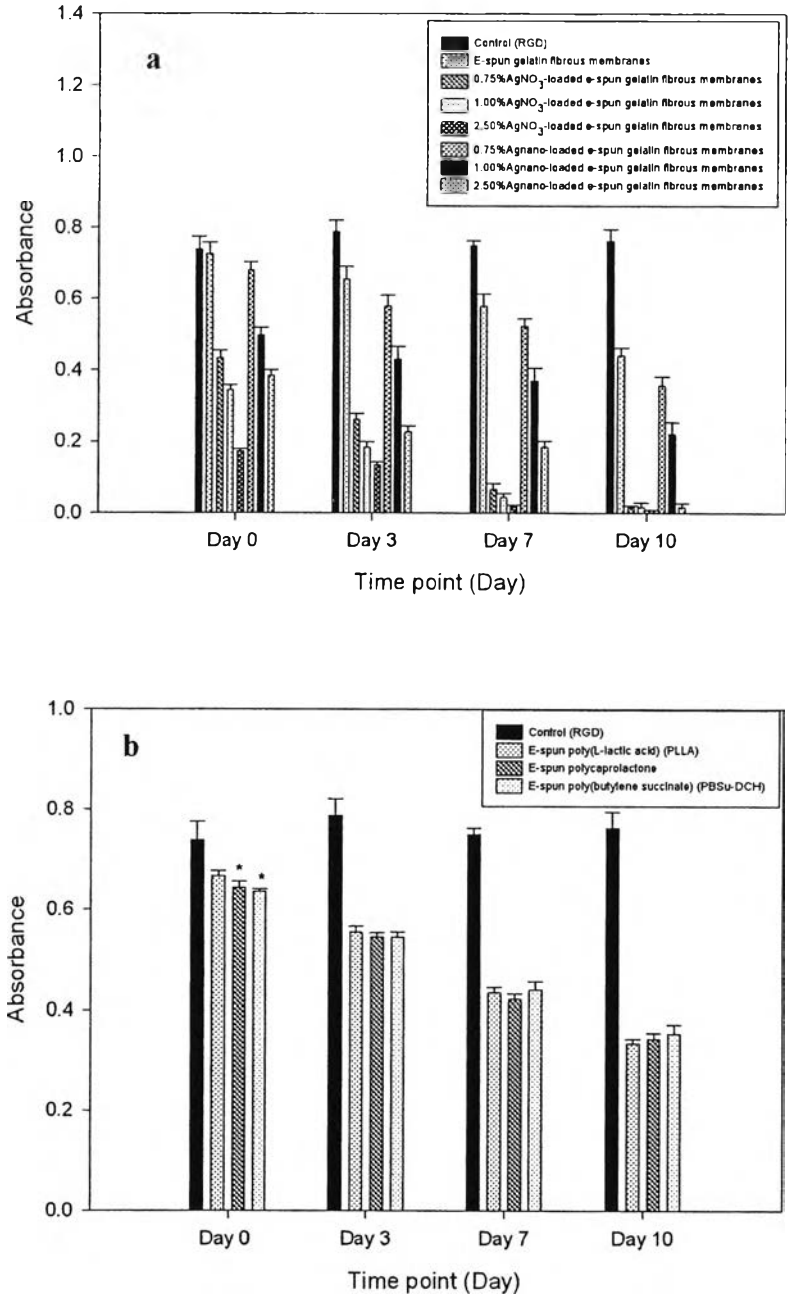


**Figure 6.1** Cell viability a) the e-spun fibrous membranes of gelatin and gelatin that contained 0.75-2.50%$AgNO_3$ and 0.75-2.50%Agnano and b) biodegradable polyesters; PLLA, PCL and PBSu-DCH as a function of time. Results are expressed as the mean of 5 experiments ± the standard error of the mean (n=5). 1, * Statistically significant vs. PLLA, $p < 0.01$.

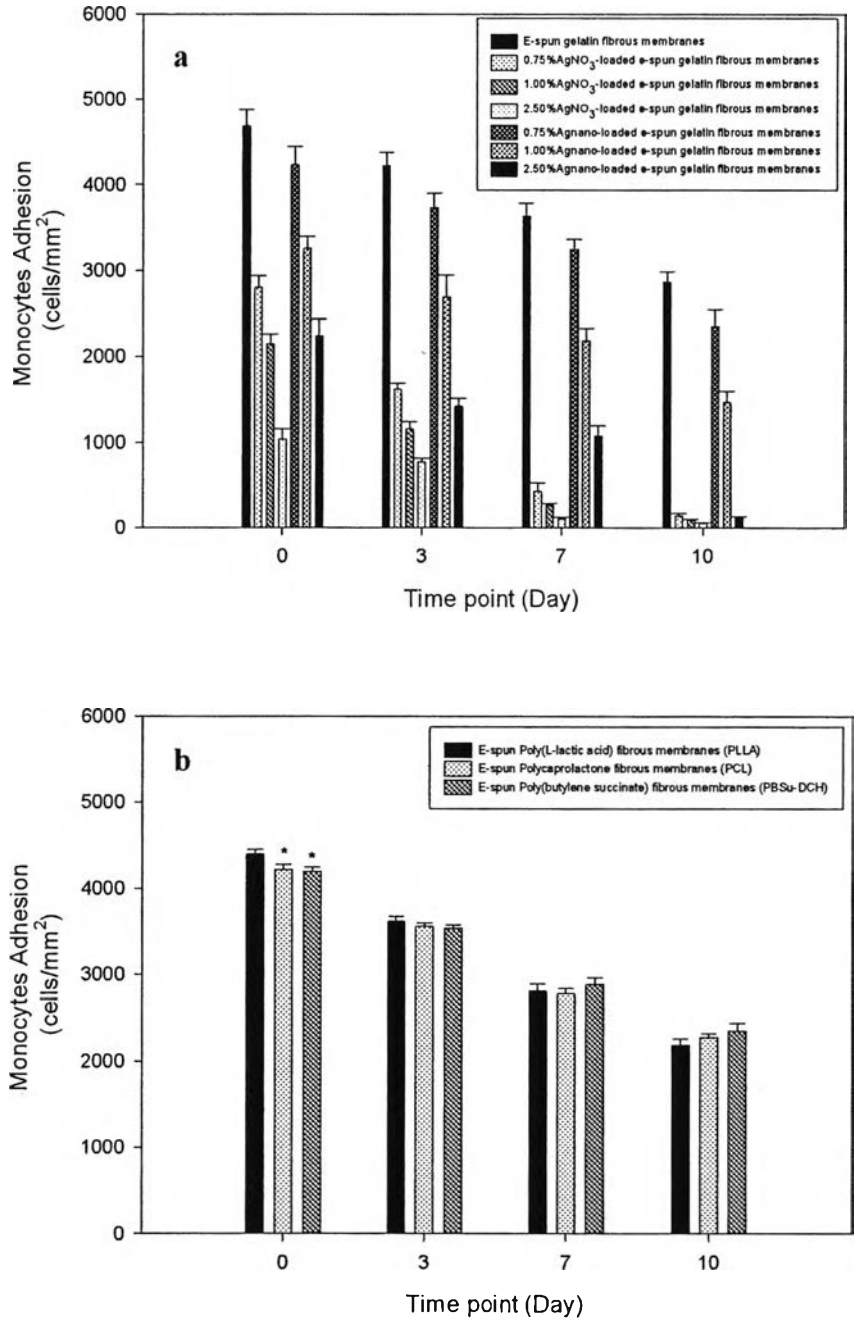


**Figure 6.2** Adherent monocyte density a) the e-spun fibrous membranes of gelatin and gelatin that contained 0.75-2.50%$AgNO_3$ and 0.75-2.50%Agnano and b) biodegradable polyesters; PLLA, PCL and PBSu-DCH as a function of time. Results are expressed as the mean of 5 experiments ± the standard error of the mean (n=5). * Statistically significant vs. PLLA, $p < 0.001$.

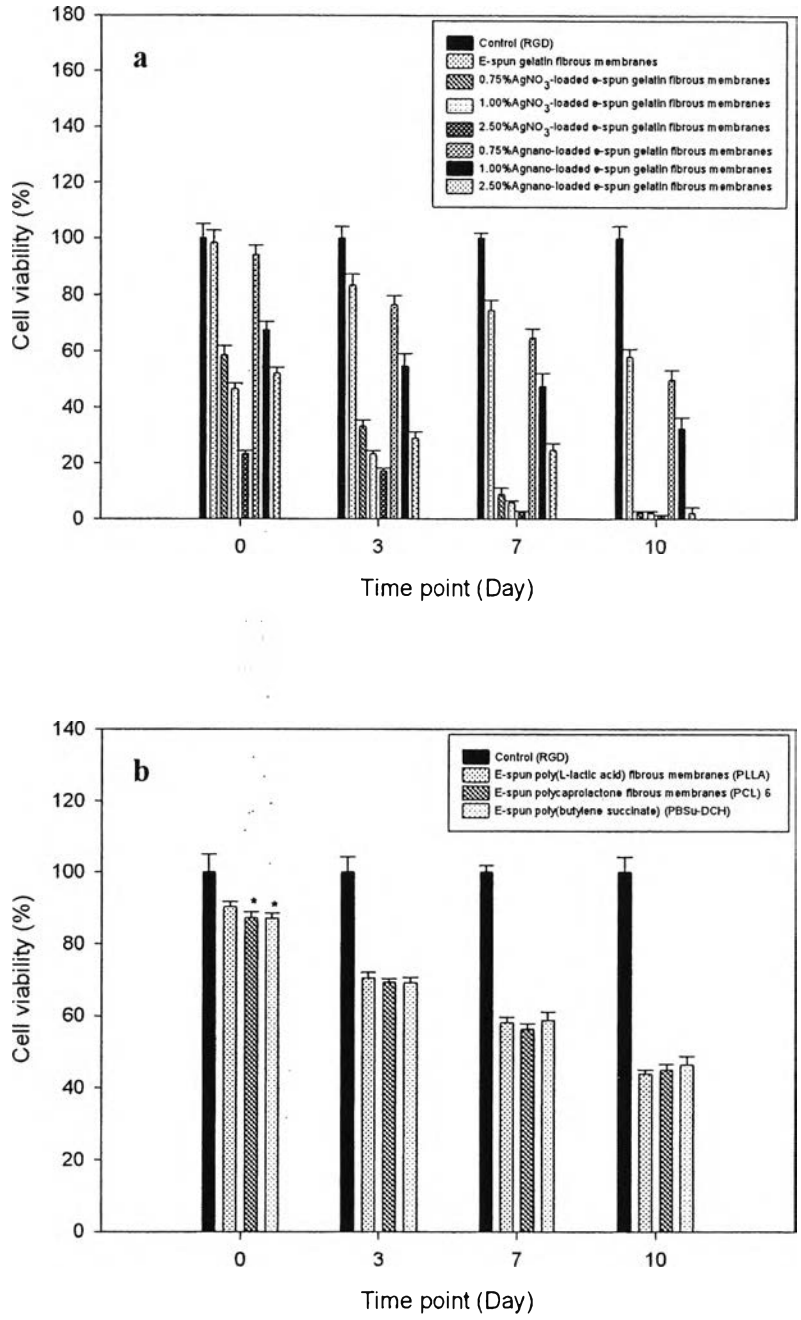


**Figure 6.3** Percentage of cell viability a) the e-spun fibrous membranes of gelatin and gelatin that contained 0.75-2.50%$AgNO_3$ and 0.75-2.50%Agnano and b) biodegradable polyesters; PLLA, PCL and PBSu-DCH as a function of the time. Results are expressed as the mean of 5 experiments ± the standard error of the mean (n=5). * Statistically significant vs. PLLA, $p < 0.01$.

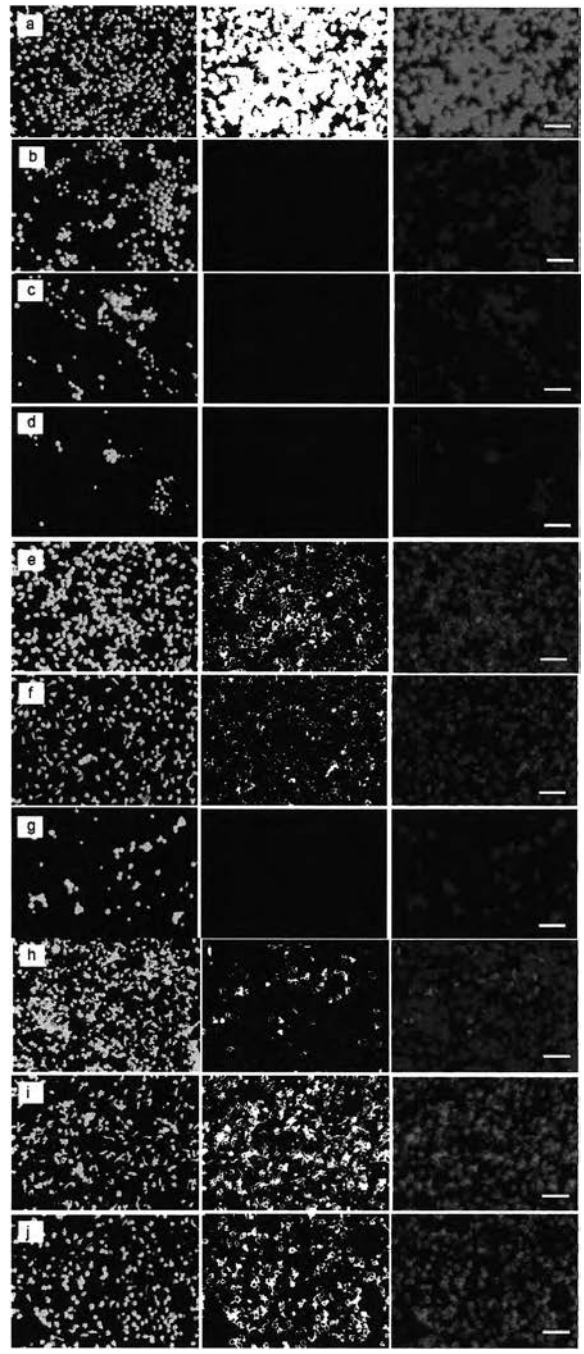


**Figure 6.4** Representative confocal images of monocytes/macrophages adhesion at day 0 (2h). Scale bar indicates 50 micrometers; (a) the e-spun gelatin fibrous membranes.; (b)-(d) the 0.75-2.50%$AgNO_3$-loaded e-spun gelatin fibrous membranes; (e)-(g) the 0.75-2.50%$AgNO_3$-loaded e-spun gelatin fibrous membranes; (h) poly(L-lactic acid) (PLLA); (i) polycaprolactone (PCL) and (j) 1,6-diisocyanatohexane-extended poly(1,4-butylene succinate) (PBSu-DCH).

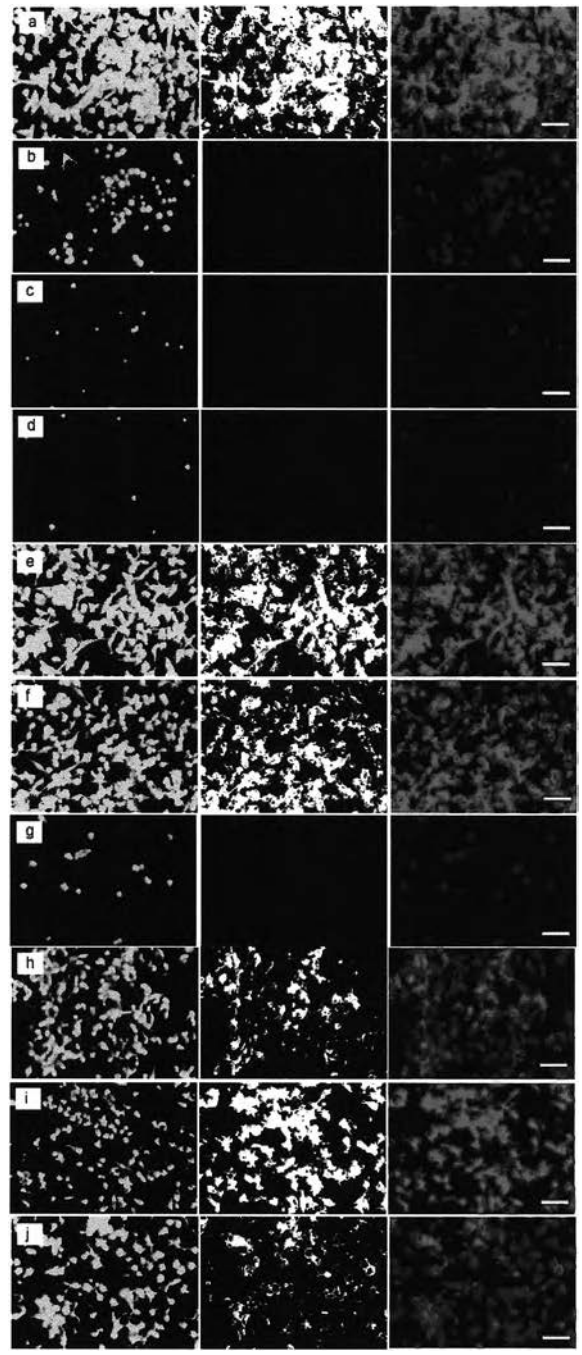


**Figure 6.5** Representative confocal images of monocytes/macrophages adhesion at day 3. Scale bar indicates 50 micrometers; (a) the e-spun gelatin fibrous membranes; (b)-(d) the 0.75-2.50%$AgNO_3$-loaded e-spun gelatin fibrous membranes; (e)-(g) the 0.75-2.50%$AgNO_3$-loaded e-spun gelatin fibrous membranes; (h) poly(L-lactic acid) (PLLA); (i) polycaprolactone (PCL) and (j) 1,6-diisocyanatohexane-extended poly(1,4-butylene succinate) (PBSu-DCH).

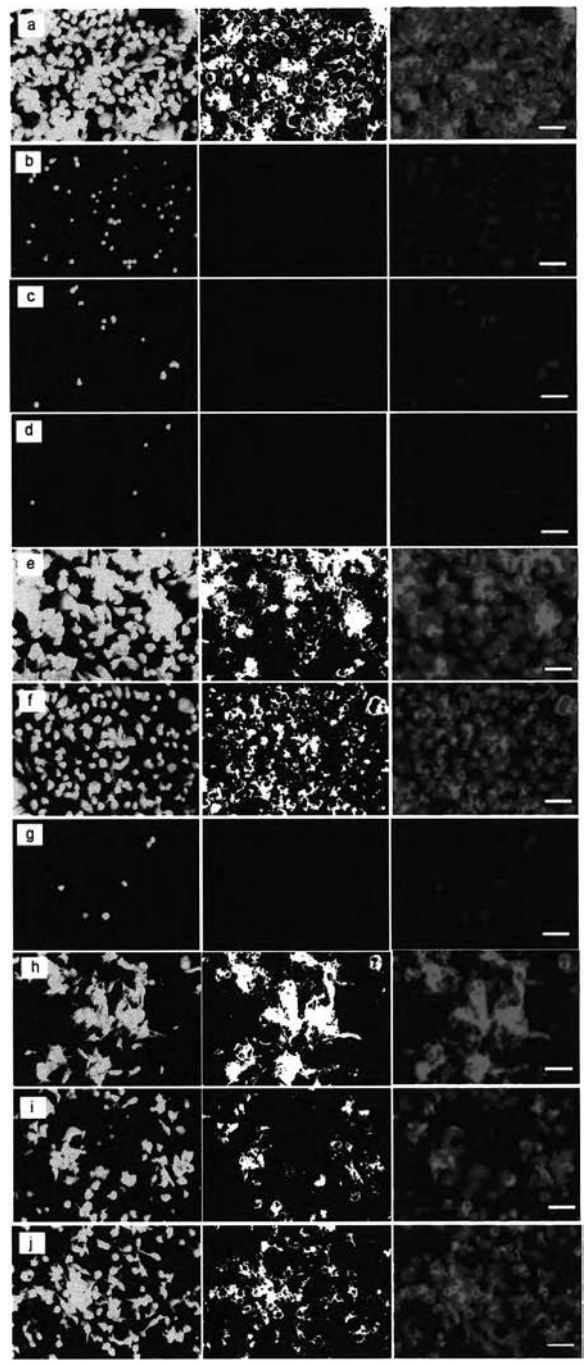


**Figure 6.6** Representative confocal images of monocytes/macrophages adhesion at day 7. Scale bar indicates 50 micrometers; (a) the e-spun gelatin fibrous membranes; (b)-(d) the 0.75-2.50%$AgNO_3$-loaded e-spun gelatin fibrous membranes; (e)-(g) the 0.75-2.50%$AgNO_3$-loaded e-spun gelatin fibrous membranes; (h) poly(L-lactic acid) (PLLA); (i) polycaprolactone (PCL) and (j) 1,6-diisocyanatohexane-extended poly(1,4-butylene succinate) (PBSu-DCH).

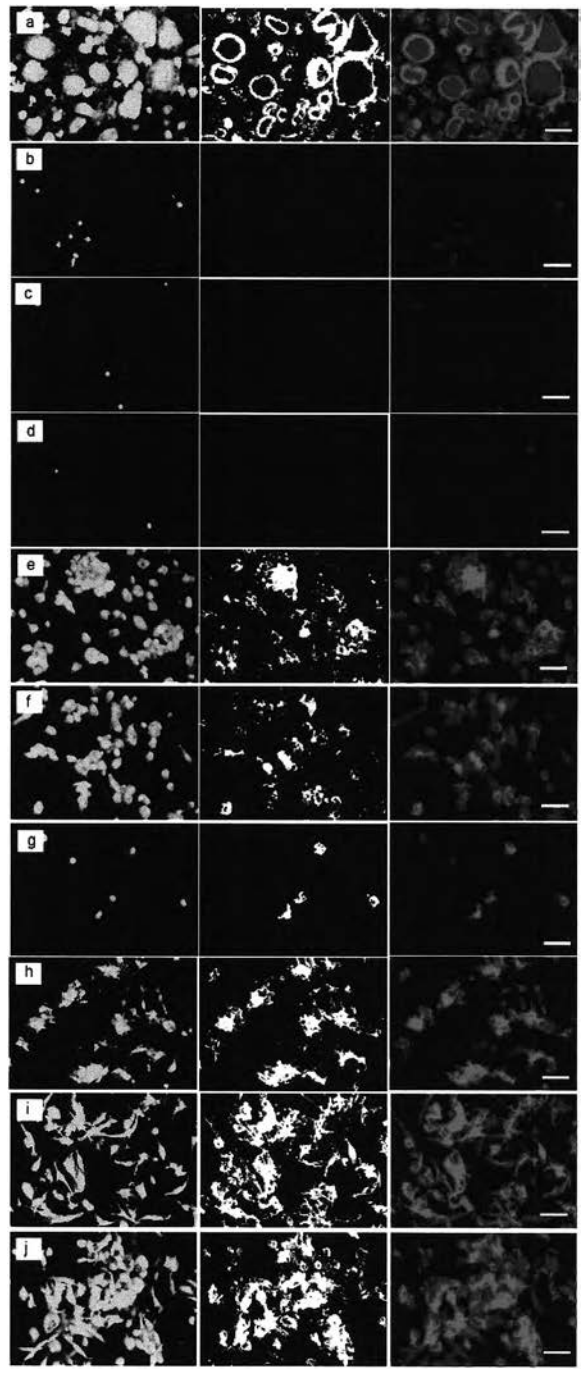


**Figure 6.7** Representative confocal images of monocytes/macrophages adhesion at day 10. Scale bar indicates 50 micrometers; (a) the e-spun gelatin fibrous membranes; (b)-(d) the 0.75-2.50%$AgNO_3$-loaded e-spun gelatin fibrous membranes; (e)-(g) the 0.75-2.50%$AgNO_3$-loaded e-spun gelatin fibrous membranes; (h) poly(L-lactic acid) (PLLA); (i) polycaprolactone (PCL) and (j) 1,6-diisocyanatohexane-extended poly(1,4-butylene succinate) (PBSu-DCH).

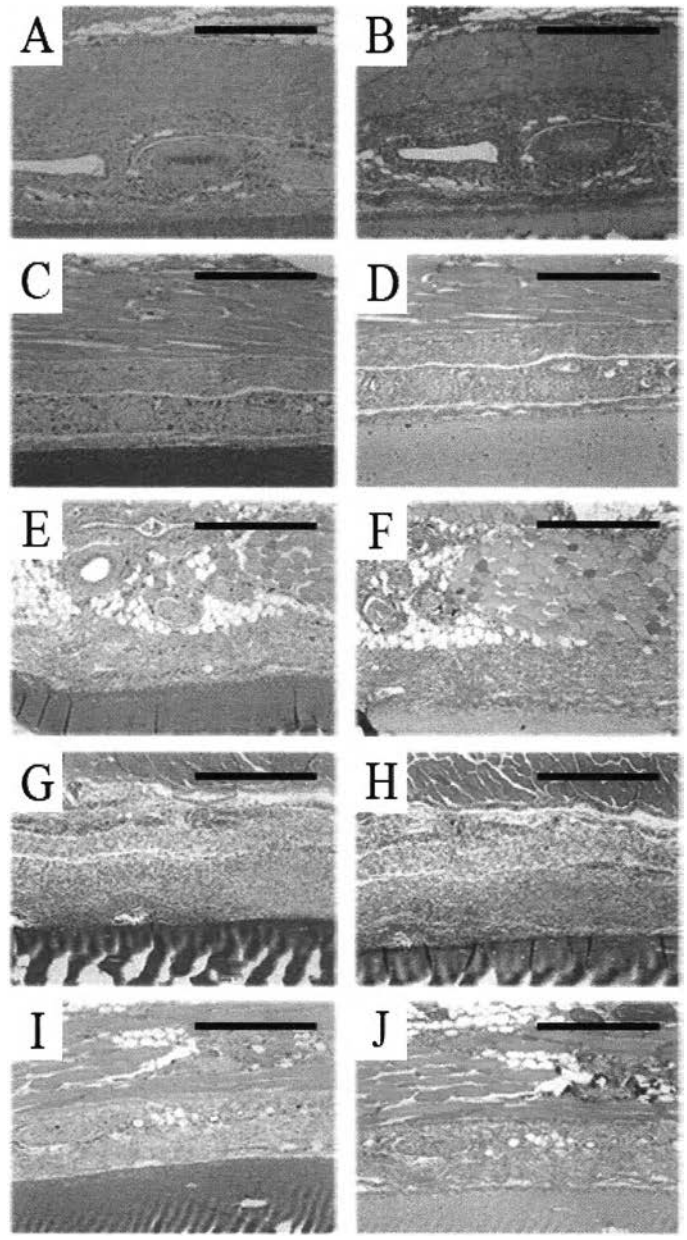


**Figure 6.8** Histology evaluation at 1 week implantation. Subcutaneous implant specimens with H&E stain for cellularity and Masson's Trichrome stain for fibrosis. Scale bar indicates 400 microns; A, B Electrospun gelatin, H&E and Trichrome; C, D 0.75% $AgNO_3$-loaded electrospun gelatin, H&E and Trichrome; E, F 1.00%$AgNO_3$-loaded electrospun gelatin, H&E and Trichrome; G, H 2.50%$AgNO_3$-loaded electrospun gelatin, H&E and Trichrome; I, J 0.75%Ag nano-loaded electrospun gelatin, H&E and Trichrome.

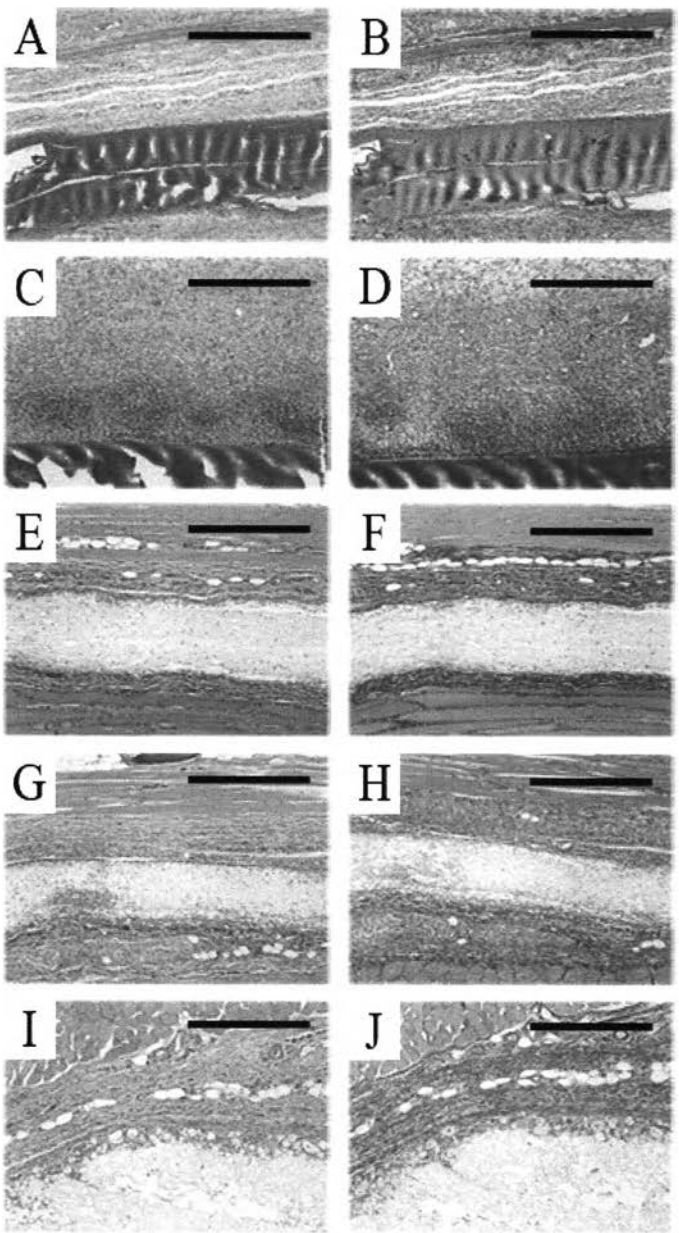


**Figure 6.9** Histology evaluation at 1 week implantation. Subcutaneous implant specimens with H&E stain for cellularity and Masson's Trichrome stain for fibrosis. Scale bar indicates 400 microns; A, B 1.00% Agnano-loaded electrospun gelatin, H&E and Trichrome; C, D 2.50%Agnano-loaded electrospun gelatin, H&E and Trichrome; E, F Electrospun poly(L-lactic acid) (PLLA), H&E and Trichrome; G, H Electrospun polycaprolactone (PCL), H&E and Trichrome; I, J Electrospun 1,6-diisocyanatohexane-extended poly(1,4-butylene succinate) (PBSu-DCH), H&E and Trichrome.

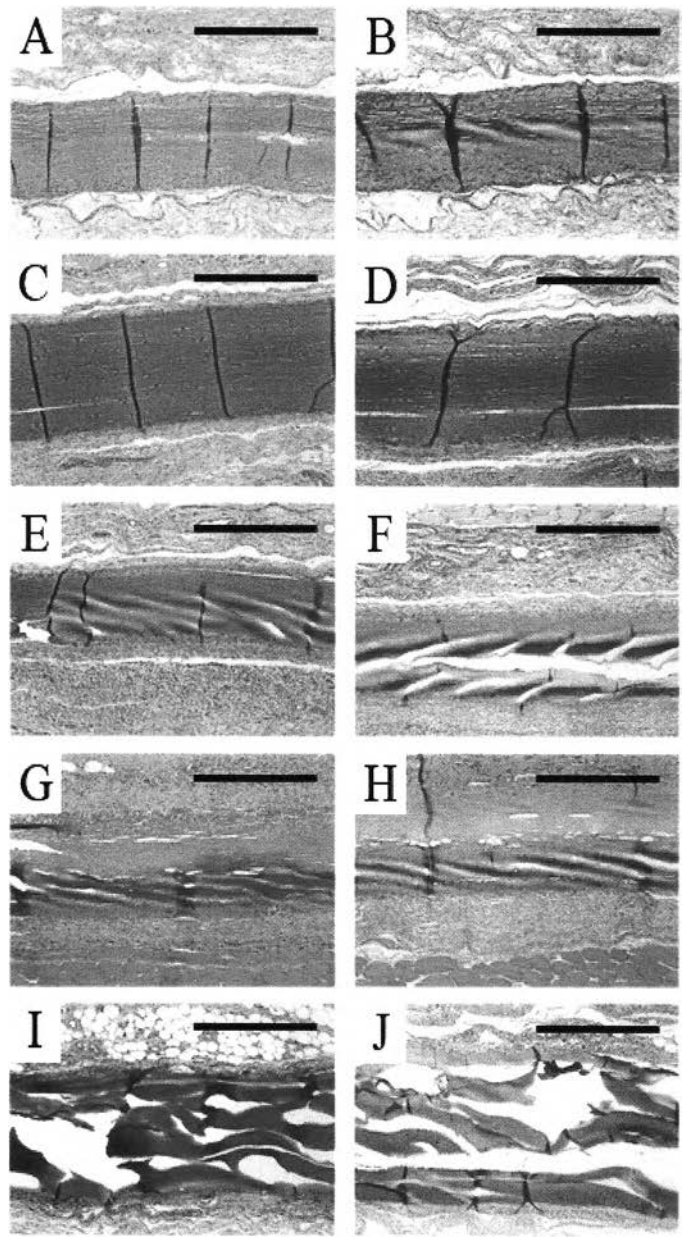


**Figure 6.10** Histology evaluation at 2 weeks implantation. Subcutaneous implant specimens with H&E stain for cellularity and Masson's Trichrome stain for fibrosis. Scale bar indicates 400 microns; A, B Electrospun gelatin, H&E and Trichrome; C, D 0.75% $AgNO_3$-loaded electrospun gelatin, H&E and Trichrome; E, F 1.00% $AgNO_3$-loaded electrospun gelatin, H&E and Trichrome; G, H 2.50% $AgNO_3$-loaded electrospun gelatin, H&E and Trichrome; I, J 0.75% Ag nano-loaded electrospun gelatin, H&E and Trichrome.

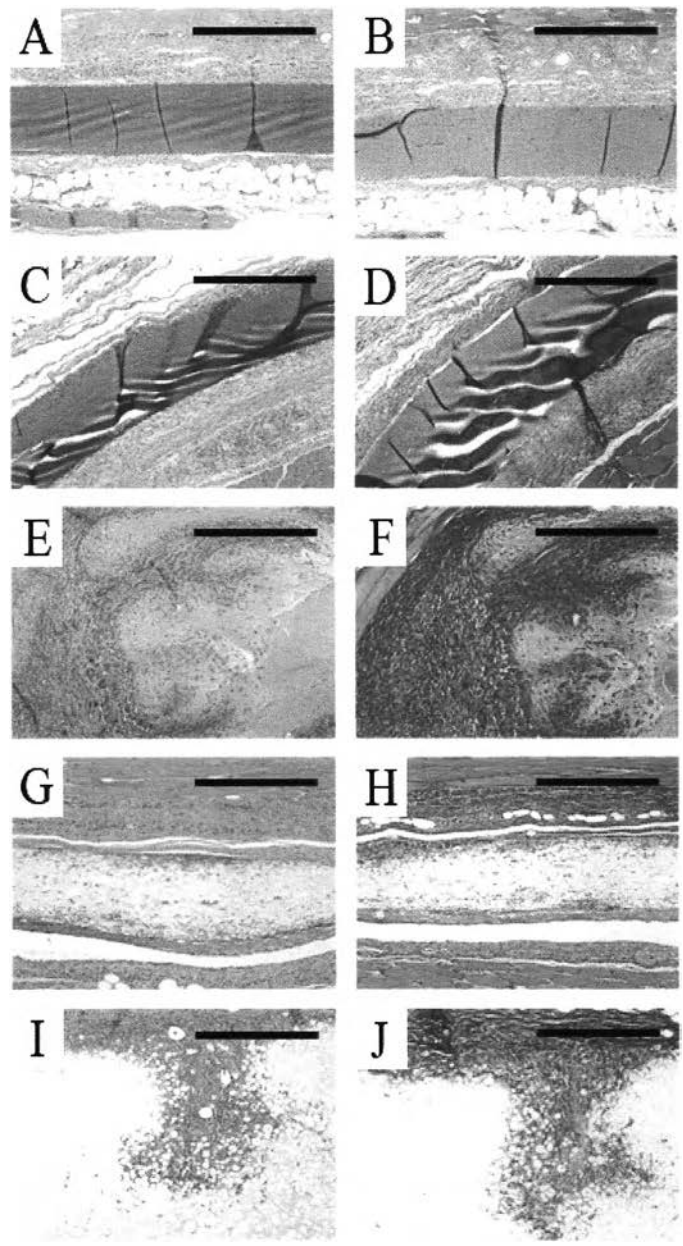


**Figure 6.11** Histology evaluation at 2 weeks implantation. Subcutaneous implant specimens with H&E stain for cellularity and Masson's Trichrome stain for fibrosis. Scale bar indicates 400 microns; A, B 1.00% Ag nano-loaded electrospun gelatin, H&E and Trichrome; C, D 2.50% Ag nano-loaded electrospun gelatin, H&E and Trichrome; E, F Electrospun poly(L-lactic acid) (PLLA), H&E and Trichrome; G, H Electrospun polycaprolactone (PCL), H&E and Trichrome; Electrospun 1,6-diisocyanatohexane-extended poly(1,4-butylene succinate) (PBSu-DCH), H&E and Trichrome.

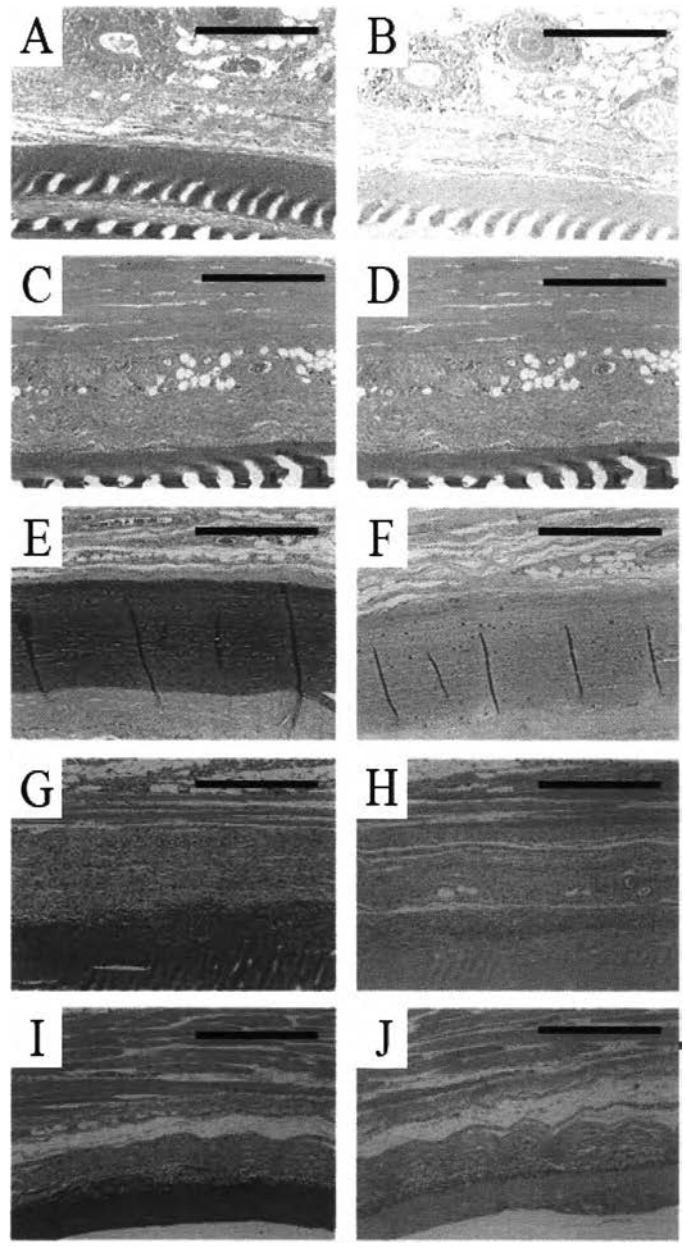


**Figure 6.12** Histology evaluation at 4 weeks implantation. Subcutaneous implant specimens with H&E stain for cellularity and Masson's Trichrome stain for fibrosis. Scale bar indicates 400 microns; A, B Electrospun gelatin, H&E and Trichrome; C, D 0.75% $AgNO_3$-loaded electrospun gelatin, H&E and Trichrome; E, F 1.00% $AgNO_3$-loaded electrospun gelatin, H&E and Trichrome; G, H 2.50% $AgNO_3$-loaded electrospun gelatin, H&E and Trichrome; I, J 0.75% Ag nano-loaded electrospun gelatin, H&E and Trichrome.

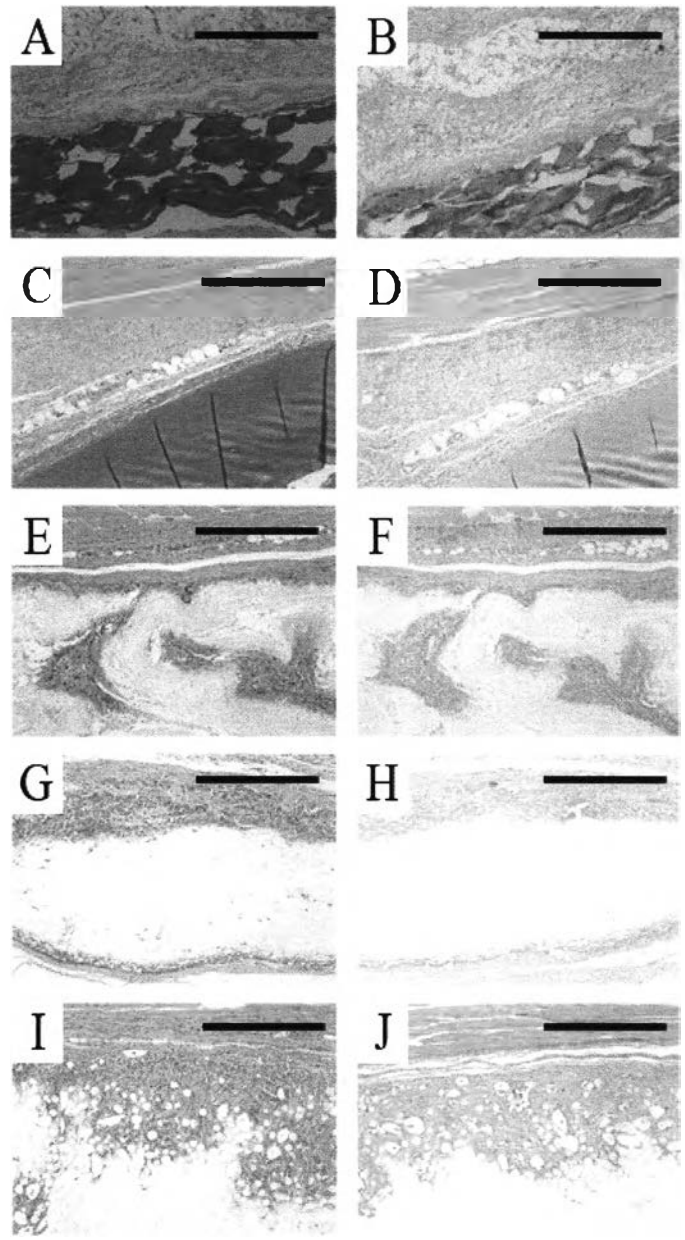


**Figure 6.13** Histology evaluation at 4 weeks implantation. Subcutaneous implant specimens with H&E stain for cellularity and Masson's Trichrome stain for fibrosis. Scale bar indicates 400 microns; A, B 1.00% Ag nano-loaded electrospun gelatin, H&E and Trichrome; C, D 2.50% Ag nano-loaded electrospun gelatin, H&E and Trichrome; E, F Electrospun poly(L-lactic acid) (PLLA), H&E and Trichrome; G, H Electrospun polycaprolactone (PCL), H&E and Trichrome; Electrospun 1,6-diisocyanatohexane-extended poly(1,4-butylene succinate) (PBSu-DCH), H&E and Trichrome.